

You et al: Methane emissions from an oil sands tailings pond: A quantitative comparison of fluxes derived by different methods

5 *Note: the line numbers given in the responses refer to those in the revised manuscript without mark-up; those in the marked-up version below are unfortunately slightly different, presumably due to comments in the margin.*

Response to comments from Referee #1

10 **We thank Referee #1 for the thoughtful comments. The specific questions and suggestions posed, in black, are answered below in blue.**

Detailed comments directed to the authors:

15 P 4 LL 119-122: You describe that a standard axis rotation was performed within Eddypro. Could you elaborate a bit more on how this rotation was performed? The abrupt terrain change can pose a problem for measurements obtained at an EC station set up at a shoreline. Especially for the wind sectors that might have contributions from land and water surface. Paw et al. (2000) and Finnigan et al. (2003) suggest considering such terrain structures in the rotation procedure of the eddy-covariance data, which can be obtained by a sector wise application of the planar-fit method according to Wilczak et al. (2001).

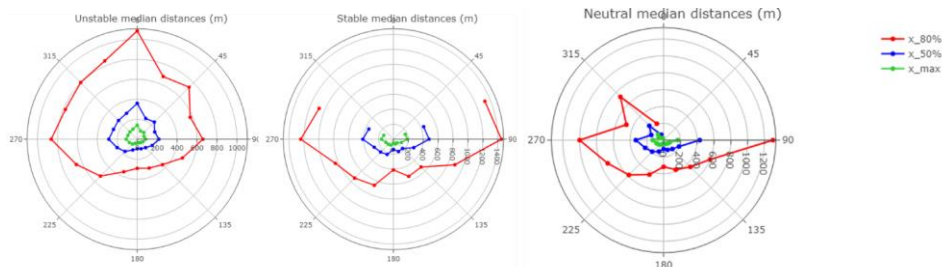
20 **Response:** We used the standard double rotation for the fluxes given in the manuscript (i.e. zeroing the average cross wind and vertical wind components). The slope of the shoreline of the pond was very gentle, and the wind was not expected to experience any significant perturbations near the flux tower. However, to evaluate the reviewer's suggestion, we recalculated the fluxes using a sector wise planar-fit method Wilczak et al. (2001). Four sectors were defined: 286° - 76° (pond sector); 76° - 124° (east shoreline sector), 124° -259° (the south sector); 259° -286° (west shoreline sector). The resulting half-hour CH₄ EC flux and the original flux were within $0.0 \pm 0.1 \text{ g m}^{-2} \text{ d}^{-1}$ of each other (mean and standard deviation of the difference). Therefore, as expected, during this campaign at this site the planar fitting method did not significantly change the final CH₄ EC flux results.

25 Section 3.2: Are there any influences of waves to be expected on the calculation of the gradient fluxes?

30 **Response:** The pond surface was mostly calm during this study. We observed that the pond surface behaved somewhat differently from natural ponds, since it was partially covered by oil slicks that suppressed wave action. Given the size and shallowness of the pond, waves would have been no more than a few cm in height and therefore insignificant even in relation to the gentle landscape features surrounding the pond.

35 Section 4.2: Could you please clarify how the shown footprint fits to the flux data set? Particularly I would find it interesting to see a separation of the footprint for the overall data set as well as unstable, stable and neutral conditions. In general an overlay of the entire footprint map over a land use map/aerial photo could provide a more useful inside to interpret the data.

40 **Response:** Thank you for the suggestion. We have added the footprint to a revised Fig. 1 and removed Figure S3. As can be seen on Fig.1, the 80% footprint contour lies completely within the liquid water surface of the pond. During this study, 98.6% half-hour periods were associated with unstable stratification when the wind came from the pond. Below, we show footprints under unstable ($z/L \leq -0.0625$), neutral ($-0.0625 < z/L < 0.0625$), and stable ($z/L \geq 0.0625$) conditions. We also included more text to describe this in Section 4.2.



50 You mentioned that one reason for the differences between chamber and EC flux calculations, is the local deployment of the chambers. One further approach to gain more information during a comparison of is to use the Kljun model to calculate the land use contribution for each half hour EC flux. This could help to understand the influence of the mentioned bubbling areas on the flux estimates.

55 Response: In the revised Figure 1, the locations of the 15 flux chamber measurements were labeled in white circles. They were all well within our 80% footprint, whereas any potential land contributions to the flux are shown by the footprint analysis to likely be insignificant. The bubbling zones on the pond surface were random and cannot simply be distinguished from inactive zones by the surface characteristics from the Google Earth image.

60 Figure S2: In my opinion it does not add much extra information since there is no clear daily pattern. Maybe a marking which direction represents the pond and land sectors would help.

Response: We agree and have removed this figure.

Response to comments from Referee #2, Kukka-Maaria Kohonen

65 **We thank the referee for this thorough review. Careful consideration of the extensive comments and implementation of many of the suggestions have made this a stronger manuscript. Below, we address each question in turn. Questions and suggestions are in black, and our responses are in blue.**

70 General comments:
Measurement methods in general require more description:

-Eddy covariance flux calculation description is lacking relevant information. The authors list as correction methods axis rotation, time lag compensation, WPL correction, and storage term correction. Which axis rotation method was used?

75 Response: More detail has been added to the manuscript (see lines 123-125 in Section 3.1). The standard double rotation (zeroing the average cross and vertical wind components) was applied (cf. Wilczak et al., 2001), and a planar fit method was tested, resulting in insignificant differences. As described in the response to Referee #1, in the test of planar fit method calculation, four sectors were defined: 286° - 76° (pond sector); 76° - 124° (east shoreline sector), 124° - 259° (the south sector); 259° - 286° (west shoreline sector). The resulting half-hour CH₄ EC flux and the original flux were within 0.0 ± 0.1 g m⁻² d⁻¹ of each other (mean and standard deviation of the difference).
80 Therefore, as expected, during this campaign at this site the planar fitting method did not significantly change the final CH₄ EC flux results.

85 WPL correction should actually not be applied for this gas analyzer (Picarro G2311-f) as it is already included in the instrument itself.

90 Response: This was indeed an oversight on our part and we are grateful to the reviewer for pointing this out. We recalculated the fluxes in EddyPro without WPL correction, and found that the new results (half-hour series) are essentially indistinguishable from our original results, with an average decrease of 0.04% lower. Therefore, this correction issue had no significant effect on our results or conclusions.

95 Spectral corrections are not mentioned in the text. Spectral corrections (especially high frequency spectral correction) are essential in EC flux processing and can affect even the sign (direction) of the flux measurement. Recommended spectral correction methods are introduced in e.g. Aubinet et al., (2000) and Mammarella et al., (2009).

100 Response: Given the measurement height of 18m, spectral corrections are usually small, which is why we did originally not apply any spectral corrections. Recalculating the fluxes and applying a high frequency correction of low-pass filtering effects according to Moncrieff et al. (1997), we found the new numbers to be very close to the old results. On average, spectrally corrected values were 0.8% higher than uncorrected values. Therefore, this correction did not significantly affect the final pond emission results and conclusions.

105 Was u* filtering applied? If yes, what was the threshold and how was it determined?

Response: We carefully investigated this issue in our early analysis, and found that there was no evidence of fluxes becoming underestimated or erratic at lower u* (Figure S4, original Figure S5). For most of the half-hour periods when the wind was from the pond, u* > 0.1 m/s.

110 How about storage change fluxes, how were they calculated?

Response: Storage fluxes of CH₄ were calculated as the second term in equation (2), i.e.

$$F_{storage} = \int_0^z \frac{\partial c}{\partial t} \partial z$$

115 Eddypro assumed that the profile was linear from the measurement point to the ground and calculated the storage flux as a separate term. In this study, the storage flux was added to the calculated EC fluxes in the final EC fluxes. Given that the dynamic stability associated with pond wind directions was in the unstable regime 98% of the time, the storage correction made little difference to the net flux.

120 Fluxes from different wind directions are presented in this study, but it is not clear weather all these fluxes were
processed in similar way. If all wind sectors are covered with different types of roughness elements (such as pond,
buildings, trees), the different sectors should be processed (and fluxes calculated) individually. Environmental data
required for the flux calculation (air pressure, temperature and humidity) are not described.

125 Response: Each half-hour flux was calculated independently, and cumulative/average statistics were calculated for
the different wind sectors to ensure homogeneous conditions upwind for each sector. Meteorological inputs were
described in lines 90-96.

-Gradient flux method has deficiencies.
130 Eddy diffusivity is calculated from CH₄ EC flux, so gradient flux is not totally independent from EC CH₄ flux
measurements. I understand the eddy diffusivity is not taken directly based on EC measurements, but from a fit of
Schmidt number against stability parameter. Even though making this fit makes gradient fluxes not directly
dependent from EC, it should still be discussed how the usage of EC measurements in eddy diffusivity calculations
affect the comparison between these methods, as it has not been currently discussed at all.
135 The authors refer to a study by Bolinius et al., 2016 where the eddy diffusivity is calculated from the heat flux
measurements of the EC system instead of the gas flux. This is a well established method and I recommend the
authors to study it more carefully and implement in their study as well. I suggest the authors at least compare this
method to their original gradient flux calculations. Another study worth taking a look at is Rantala et al., (2014),
where eddy diffusivity is calculated from the Monin-Obukhov similarity theory. Heat flux is independent from the
gas flux, so calculating eddy diffusivity from the heat flux measurements will allow more reliable comparison
140 between EC and gradient CH₄ fluxes.

Response: We evaluated the method of using the heat fluxes to establish an eddy diffusivity K_T early on, but found
these diffusivities to be significantly noisier than those based on momentum. And an obvious problem with using
heat fluxes as a baseline is that fluxes are very small at night, and therefore K_T becomes very erratic and unusable.
145 K_m is also independent of the gas fluxes and has the advantages of being relatively well-behaved and continuous.
There are similarities between our approach and that of Rantala et al (2014), but our approach does not rely on
Monin-Obukhov Similarity Theory since we use the directly measured momentum flux, and the stability corrections
that are explicit in the M-O approach are incorporated into our formulation of the Schmidt number.
150 We are well aware that our gradient fluxes are not truly independent of the eddy covariance fluxes. However, the
fact that the Schmidt number we calculate agrees with previously published constant serves as an independent
verification of the gradient flux approach. Even using a constant Schmidt number and stability corrections from
literature, i.e. not using the measured EC methane fluxes at all, would have produced very comparable gradient flux
numbers.

155 - Chamber measurements are currently not described at all but a proper method description is needed (what kind of
chamber design was used, dimensions, how long enclosure time was after reaching equilibrium with carrier gas flow
and inside air, how was the air flow implemented, how was the flux calculated, what kind of data selection methods
were used etc.).

160 Response: The chamber measurements, which were performed by a third party independent of our project, followed
the US EPA Standardized point measurement technique (adapted from Kienbusch, M., Measurement of Gaseous
Emissions rates from Land Surface Using an Emission Isolation Flux Chamber, User Guide, EPA Users Guide,
Contract No. 68-02-03389-WA18 (EPA/600/8-86/008), 1986. Regulations regarding chamber measurements in
Alberta are given in <https://open.alberta.ca/publications/9781460145814>. The key steps are reproduced here:

165 1. Once the flux chamber (~0.1m² surface coverage area) is deployed on the target surface of interest, the valve
of nitrogen cylinder was opened to begin purging the flux chamber with 99.9995 percent pure nitrogen gas. The
flow rate of the nitrogen sweep gas was adjusted to a certain flow rate using the rotameter and this rate was
maintained throughout the sample duration. The exhaust gas sample/purge rate did not exceed 2.5 L/min. This
prevented ambient air entraining into the chamber and maintained a minimum exhaust rate 2.5 L/min out of the
pressure equalization port. The GHG analyzer has an internal pump that operates at 0.5 L/min. The start time of the
170 purge and the initial concentrations of CH₄ were recorded on the field data sheet.

2. For the first 45 minutes, concentration readings were noted on the field data sheet in 15-minute intervals.
Approximately five times the flux chamber volume was be purged in the first 45 minutes of sampling. Generally, the

175 CO₂ and CH₄ concentrations reached steady-state 30 to 45 minutes into purging as indicated by a plateau in the real time data curve.

3. After 45 minutes, concentration readings were recorded every 10 minutes for a minimum of 75 minutes of total sampling duration. A minimum of 30 minutes of steady-state concentration data had to be obtained for the sample to be valid. The recorded concentrations and times on the field data sheet act as a back up to the GHG analyzer data files.

180 Comparison of fluxes is highly misleading and fundamentally flawed. The authors have included in the flux averages all data available, which are then compared with each other. What the authors should do instead is to select only those time periods/data points when all the measured fluxes are available, and then calculate averages that are comparable. If this is not done, it easily happens so that one of the methods is measuring e.g. more fluxes from one wind direction or time of the day than the other, which is causing a clear bias in the comparison.

190 Response: We have added text to clarify that the comparisons we show for the EC fluxes, gradient fluxes and inverse dispersion model fluxes are of course based on the set of simultaneous half-hour measurements over the 5-week study, when data was available to calculate all three. This does not apply to the comparison with the chamber fluxes, since the flux chamber measurements, conducted by a third party, happened to be performed when the wind was from the south and the micrometeorological methods (located on the south shore) could not observe the pond. For this comparison, the assumption is made that emissions from the pond are relatively time invariant during the period that was missed by the micrometeorological fluxes, as supported by the time series of fluxes for wind directions from the pond during the study period. This is in fact a common assumption made in many applications of flux chamber work, due to the snapshot nature of such measurements, and represents a significant limitation of flux chambers that we highlighted in lines 44-48 and in section 4.6 and 4.7. These well-known limitations were one of the reasons for exploring alternative methods for quantifying fluxes from such sources of fugitive emissions.

200 Conclusion section is currently an additional discussion section that should have been implemented in the section "Results and discussion" already. Proper conclusions – with no new information given but rather a summary with a perspective to future studies – is totally missing and should be included.

Response: A conclusion section has been added, and a comparison to previous results was inserted into Section 4.7.

205 Specific comments:

Table 1: This comparison does not make sense if the fluxes are not averaged from simultaneous measurements. You should only include the datapoints in averaging when you have a datapoint from all the methods. What does it mean that fluxes are "relatively steady"? The uncertainty estimation in footnote c is unclear.

215 Response: As explained above, the comparison of EC flux, gradient flux, and IDM flux is of course based on a set of simultaneous half-hour data points, when data was available to calculate all three, with wind directions from the pond. The exception are the flux chamber results, for which an assumption of time invariant fluxes during the concurrent micrometeorological flux time series is required.

220 The uncertainty estimation is based on a conservative, integrated approach encompassing all errors. In the real data time series, periods were identified when the flux did not fluctuate much, i.e. represented steady state conditions. In this case, we found in EC flux time series five periods of at least five half-hours with standard deviation not greater than 0.89. Then, the average of the standard deviations from these five periods was used as the uncertainty of EC flux in this study. For gradient flux and IDM flux, we used the same five periods, and calculated the average of the standard deviations from the five periods. This approach provides an upper limit or conservative estimate of the overall uncertainty in the final flux.

225 Table 2: Not clear what are the time periods for these flux estimates, should they even be comparable? Annual averages are different from summertime measurements. It would be interesting to see a comparison to natural waters or reservoirs as well, to see the high magnitude of the methane emissions.

Response: We are comparing all data available publically for this particular pond. The Small et al. (2015) data were from measurements in 2010 or 2011. Stantec report (2016) data were from measurements in 2013 and 2014. Baray

230 et al. (2018) results were from the aircraft campaign in 2013, which was discussed in Section 4.7. These data were
compared to provide context of results from this study. The comparison of annual averages vs. summertime
measurements was discussed in Section 4.7, in the first paragraph.
Natural lakes and indeed even wetlands emit at rates well below what we observed on this industrial pond, typically
on the order of 0.005-0.05 g m⁻² d⁻¹ (Sanches et al., 2019).

235 Figure 1: It would be very helpful for the reader to include in the map the EC footprint lines and/or lines for
approved wind directions. It is not very clear from the closeup image where exactly are the pond edges. Maybe this
could be highlighted somehow? Add chamber measurement locations to this map.

240 Response: Yes, the EC footprint lines and chamber measurements have been labeled in the revised Figure 1. A
sentence has been added to the caption explaining the different shadings of surface cover.

Figure 2: What is the correlation coefficient of the linear fit? How does it change if you use the original datapoints
instead of binned averages for fitting? It does seem that data are very scattered with higher Km and Kc, how does
245 this affect the fitting? What do the boxplots represent (what are the box limits, whiskers, center line etc)?

Response: The correlation coefficient for the linear fit was $r^2=0.93$. The original data points were indeed quite
scattered, but produce the same slope. The figure caption has been revised to label box, lines and whiskers.

250 Figure 3: “Best fit” - determined by what criterion? The bins are not of equal size and I believe this is also affecting
the fit. What do the boxplots represent (what are the box limits, whiskers, center line etc)?

Response: Bins are actually of equal size with bin width = 1, except for the last bin on the right for $z/L > -0.34$. At
 $z/L=0.34$, the exponential is equal to the $Sc=0.923$ found from the linear fit in Fig. 2; therefore, this was chosen as
255 the point to switch from the exponential to the constant part of the function.

Figure 4: Fig 4b is not discussed anywhere and is a bit pointless without water temperature. In 4a, u^* is missing
interquartile ranges and 10% and 90% percentiles. In 4e sensible heat flux is missing quartiles off-pond and 10%
and 90% percentiles on pond. Mark in the diurnal plots the times of sunset and sunrise to help the reader.

260 Response: All the information required is shown; from the temperatures in panel (b) and the temperature difference
shown in (c), the absolute pond surface temperature can be inferred if desired. Panel (b) was in Figure 4 to show the
typical diurnal cycle of ambient temperature. We have now cited panel(b) in Section 4.1.
The figure has been revised to include sunrise, sunset and off-pond heat flux quartiles.

265 Figure 5: Scale seems quite arbitrary, how was it defined? Directions are missing, where is north?

Response: The scale was set to include roughly equal numbers of data points in each range. The figure caption has
been revised to label north.

270 Figure 6: You should add a, b and c to subplots. Colors of EC and gradient fluxes are too similar in the printed
version and in the lowest panel red and green are used which is not color-blind friendly. You can check colorblind
and printer friendly color choices e.g. from here: <https://colorbrewer2.org>

275 Response: Fixed.

Figure 7: Shade the pond area also here, similar to Fig. S6. What do the boxplots represent (what are the box limits,
whiskers, center line etc)?

280 Response: Shade has been included here. Lower and upper bounds of the box plot are 25th and 75th percentile; the
line in the box marks the median and the black square labels the mean; the whiskers label the 10th and 90th
percentile.

285 Figure 8: What is the offset of the fit? It does not seem to be crossing $y=0$ at $x=0$ in neither of the plots.

Response: They both indeed cross (0,0).

Figure S2: What do the confidence intervals represent?

290 Response: The blue shade is 25th percentile to 75th percentile of the wind direction in degrees. This figure shows that
the diurnal variation of wind direction is weak. However, this point can be made in the text without a supporting
figure, as suggested by the other reviewer, and we decided to remove this plot.

295 Figure S3: "...countours of the EC footprint area". It would be very helpful for the reader to get S3 b on top of a
map, to see where the contours are crossing pond edges.

Response: We agree. The footprint contour is now superimposed onto the pond map in the revised Figure1.
FigureS3 has been removed.

300 Figure S4 (now S2): It is not mentioned here which EC flux this is. Methane? Mention in each subplot which wind
direction it is representing (in legend/title/xlabel/ylabel) to help the reader. What do the boxplots represent (what are
the box limits, whiskers, center line etc)? Mention in the caption what is in each wind sector (pond, buildings, trees,
etc).

305 Response: Yes, we mean methane EC fluxes. All these suggestions are accepted and Figure S2 has been updated.
Lower and upper bounds of the box plot are 25th and 75th percentile; the line in the box marks the median and the
black square labels the mean; the whiskers label the 10th and 90th percentile.

310 Figure S5 (now S3): Mention in the ylabel that this is methane flux. Mention in the caption what is the r2
representing (least squares linear fit?).

Response: Caption has been revised to note r².

315 Figure S6 (now S4): What do the boxplots represent (what are the box limits, whiskers, center line etc)?

Response: Caption has been revised.

Figure S7 (now S5): What do the boxplots represent (what are the box limits, whiskers, center line etc)?

320 Response: Caption has been revised.

Table S1: Are the fluxes compared here from exact same time periods? Same comment as for Table 1 about the
uncertainty estimate and "relatively steady".

325 Response: Yes, the CH₄ gradient flux with variable Sc and constant Sc use exactly the same vertical mole fraction
gradient data over exactly the same set of simultaneous data. An explanation of the uncertainty estimate was given
in our response to comments on Table 1 above.

330 L10: "develop" is a little bit misleading here since the authors don't really develop any
new method, rather compare already existing ones.

Response: While all three micrometeorological methods are of course well established, we are not aware of any
previous instances of our approach of calculating the gradient fluxes through the use of a momentum flux diffusivity
adjusted with a stability-dependent Schmidt number. Therefore we would like to keep the current term.

335 L11-12: Mention briefly which are these three flux methods in one sentence.

Response: Done.

340 L15: inverse dispersion model comes here from out of the blue. Describe it briefly before writing about the results.

Response: Done. The Inverse dispersion model is now introduced in line 12. A detailed explanation of the method is given in section 3.3.

345 L18-19: This sentence is a bit misleading. In one perspective it is quite obvious that a larger footprint represents a larger area. On the other hand if the EC tower is placed so that it is measuring only e.g. shallow area while actually the pond is deeper from a much larger area, then would EC be representative of the whole pond emissions? Then on the other hand nobody can know what is the real flux. It might as well be closer to the chamber flux than EC.

350 Response: There are several reasons that point to the eddy covariance fluxes being the more accurate estimate of the true fluxes. We have shown that fluxes were consistent for various wind directions across the pond, over a month of measurements, and they represent a large fraction of the pond surface. This is in contrast to the chamber measurements which cover a total of a few m² for instantaneous snapshot measurements, limited to regions of the pond accessible by boat. Implications have been discussed in the manuscript section 4.6 and section 5. Also of concern is the large interannual variability in flux chamber results, with 5.3 g m⁻² d⁻¹ in 2016, 2.8 g m⁻² d⁻¹ in 2017 and 11.1 g m⁻² d⁻¹ in 2018, despite similar operational conditions.

L21: Abbreviation AOSR is not used anywhere in the text

360 Response: Deleted.

L23: “Oil Sands” or “oil sands”? Throughout the manuscript.

Response: Made “oil sands” consistently throughout.

365 L48: “eddy covariance (EC)” and then use EC after this throughout the manuscript instead of eddy covariance

Response: Fixed.

370 L49: “area sources” or “source areas”?

Response: Area sources

L53: So only emissions can be measured with this method, not uptake?

375 Response: Uptake can of course be measured too, and would manifest itself as a negative flux. The two cited studies were emission flux studies.

380 L56: What is meant by “relatively well-defined spatially”? If the fluxes are well-defined, why do you measure them?

Response: We meant that the source area was relatively well-defined spatially, not that the fluxes were known. The ponds cover a well-known spatial domain, in a remote region far from urban activities and other sources.

385 L59: “Field study” is not a very descriptive title. Maybe “Site and measurement description”?

Response: Agreed & implemented.

390 L62: Trees are not part of natural landscapes? What is? How far were the other facilities? In the catchment area or further away? How large is the catchment area?

Response: This artificial pond is elevated above the surrounding landscape and has minimal catchment (~ 100m around the shoreline). The influx of industrial processed water vastly dominates the water budget of the pond. We added distances to the main facilities nearby to the text in lines 62-65.

395 L65: What is meant by “mobile tower”? How high were the measurements above water (which is more relevant than ground in the case of pond fluxes)?

400 Response: The tower mounted on a truck bed and can be easily towed from place to place for temporary installations. The base of the tower was less than 30cm above the water surface.

L69: Is this the diameter or radius? Inner or outer diameter?

405 Response: Outer diameter. This is now noted in line 73.

L71-72: I am not sure it can be said that turbulent flow is ensured. Reynolds number is ≈ 1300 according to my calculations, so it is possible that the flow is turbulent, but I wouldn't call it "ensured".

410 Response: Teflon tubing is generally labelled by outside diameter. Calculating the Reynolds number with the inside diameter of (3/8" minus wall thickness 1/16") $D = 0.635$ cm, with a flowrate of $Q = 117 \text{ cm}^3 \text{ s}^{-1}$ and a kinematic viscosity of $\nu = 0.148 \text{ cm}^2 \text{ s}^{-1}$ gives $Re = (Q D)/(\nu A) = 4500$, well within the turbulent regime.

415 L72-74: All kinds of measurements are presented that are not used in the analysis or shown anywhere in the manuscript. I suggest to leave out the description of those gas measurements not used in this particular study. Why is a 40 m long tubing required for 18 m height measurements? This will cause quite long lag time for EC. What are the three and four levels mentioned here?

420 Response: 40m tubing was used for all gradient levels including the 18m height measurement, to avoid systematic differences due to tube lengths. Three levels was a typo; the G2204 sampled from four levels, 8m, 18m, 32m on the tower plus 4m on the roof of the trailer. The length of the EC 3/8" OD line was 30m; this has now been added to the manuscript. We have removed the description of the G2401-M analyzer since its data was not used in this work.

425 L74: There must be some flush time of the tubings and analyzer between the different height measurements. How long is the flush time? One level cannot be measured 2.5 min during 10 min period if you take into account the flush time.

430 Response: Air was drawn through all 4 tubes continuously, and the only part of the flow system requiring flushing was the last 4m of tubing. To allow for the flow and pressure to equilibrate after each level switch, the first 30 s of the 150 s period at a given level were eliminated from the averaging process.

L76-77: Was there any drift of the instruments between calibrations? Did they compare well with each other?

435 Response: The calibration coefficient (slope) for CH_4 changed by 0.12% from before to after the study, and the offset by less than 0.002 ppm.

L80-82: This is well known EC theory and does not need to be explained.

440 Response: Since this information is fundamental to this paper and not all readers of this journal may be familiar with it, we chose to retain this.

L88-89: Was the infrared sensor calibrated somehow?

Response: No.

445 L92: How were the suitable wind directions determined?

Response: They were based on the map.

450 L104: EC also has its limitations, "benchmark" seems a bit exaggerated

Response: We have changed "benchmark" to "reference".

455 L106: Response time and sampling frequency are not the same. Response time should be given in seconds, sampling frequency in hertz. EC measurements require both fast response times and high sampling frequency.
Response: Fixed.

460 L107: “CO₂ and CH₄ fluxes”
Response: Fixed.

465 L108-109: Reformulate the sentence. EC does not calculate anything, and in this case you are talking about gas fluxes explicitly (not e.g. heat flux since you mention mole fraction)
Response: “method” is inserted after “eddy covariance”.

470 L113-114: Repetition from above
Response: Modified.

475 L115: “storage change flux”. Out of curiosity, how large was the storage change flux? Often in lake studies they have been neglected but might be important as well.
Response: CH₄ storage fluxes was small. When the wind was from the pond, the storage flux was -2% to 3% (interquartile range) of the first term in equation (2).

480 L118-122: More description is needed on the processing methods used. How long was the lag time on average?
Response: More description has been inserted.
Covariance maximization method was used in time lag compensation. This method maximizes the covariance to variables (Fan et al. 1990), within a window of plausible time lags automatically calculated by EddyPro. The lag time on average was 12 second. (Fan et al., 1990).

485 L122: What do the different flags mean (what are the criterion)?
Response: As described in Mauder et al. (2016) and Mauder and Foken (2004), the quality test calculates the ratio of the standard deviation of CH₄ flux to CH₄ flux. Then, this ratio (or relative standard deviation) is compared to modelled results (as described in Mauder and Foken (2004)) to get a relative difference. The flags are determined based on this relative difference. In this study, we used the widely used overall flag system also described in Mauder and Foken (2004): flag = 0 when this relative difference < 30%, flag = 1 when 30% < this relative difference < 100%; and flag = 2, when this relative difference > 100%.

495 L123: “Gradient flux method”
Response: Fixed.

500 L130: units?
Response: Unit of K_c are m²s⁻¹

505 L135: How do you define the gradient method footprint?
Response: This was mentioned lines 136-137 and explained in detail in the footprint section (4.2).

L168: Shifting winds are also a problem for EC measurements!

510 **Response:** That is correct. Since shifting winds are a problem for both methods, our way of excluding fluxes when the signs of EC flux and gradient fluxes were opposite at least partially excluded such situations from the comparison.

L177-180: What are the units of these variables?

515 **Response:** In this study for CH₄, unit of C and C_b is ppm, unit of Q is g m⁻²day⁻¹. However, the formulation is valid for any consistent system of units desired.

L181: Why are L and u* used as inputs, since u* is already used in calculating L?

520 **Response:** To quantify stability, u* by itself is insufficient, and the heat flux is also required, as incorporated in the Obukhov length L. Since L was already defined in the previous section, stating the inputs in this manner seemed the least confusing option to us.

L185: How close is “right beside”?

525 **Response:** Fixed. The new sentence “CH₄ mole fraction input was taken from the OP-FTIR measurement which was located 10m to the east of the flux tower.”

L188-195: More description needed

530 **Response:** Yes, we have inserted more details. The full details are available through the Alberta online public report cited, and are not the focus of this paper.

L196-199: Not understood where this is used (which methods) and why. More description please.

535 **Response:** The standard method for flux chamber operations for compliance monitoring in Alberta was used. The details can be found in the online report cited in Section 3.4. Please also see the response above for the chamber measurements.

L202: “wind coming from” or “wind that came from”

540 **Response:** Changed to “coming from”

L214: Sunsets and sunrises are not directly seen from Fig 4d.

545 **Response:** Fixed. The revised Figure 4 now has yellow shades marking the range of sunrise and sunset times for the study.

L215-216: The same wind direction/ source area applies to gas fluxes. Why different wind direction analysis is applied to sensible heat fluxes and not the others?

550 **Response:** This section was talking about meteorological parameters. All fluxes, including sensible heat fluxes and gas fluxes, were analyzed in the same manner. Results in Table1 are based only on data associated with wind directions from the pond.

555 L229: You can only see this from Fig 4c. What is meant by “species”? Methane?

Response: This applies to all species emitted from the pond, not just CH₄.

L225-230: This is done for wind direction filtered data I assume? Should be clarified since all wind directions are analyzed in some way or another in this manuscript.

560 **Response:** This has been done for the all half-hour periods. The footprint polar plot shows the footprint under unstable conditions. This is noted more clearly now in the revised Figure 1 caption.

565 L230: This is not seen from Fig S3 (b), since you cannot see pond edges in the figure.

Response: Fixed, in the revised Figure 1.

570 L231: “gradient flux”

Response: Fixed.

L234: delete “however”

575 Response: Fixed.

L235-240: But there is much more data from off-pond direction than from pond direction. How does influence the analysis?

580 Response: That was the reality dictated by uncontrollable constraints such as site accessibility and weather, and one reason for scheduling a 5-week long campaign, to ensure a statistically significant number of days for most wind directions. There were 280 half-hour periods when the wind was from the pond and 98.6% of them were under unstable conditions, i.e. our footprint results have reasonable statistics.

585 L245-253: It is not clear why fluxes off-pond are reported since this is a study concentrated on pond emissions. Are these sectors processed in flux calculation individually or not?

590 Response: All the sectors were processed in the same way in EddyPro calculation. Off-pond fluxes were reported here to provide a measure both of the methodological noise in the signal, as well as the background (non-pond) flux magnitudes. Off-pond fluxes are either close to zero, or had a slight increase during the middle of day. The pond fluxes had no significant diurnal pattern.

595 L253-258: Are these now results from pond direction? Wind and turbulence are still driving the turbulent/diffusive transport of gases from pond to the atmosphere (e.g. Tedford et al., 2014).

600 Response: Yes, fluxes from pond direction. The pond flux diurnal cycle was shown in Figure S4(a). In the main manuscript we state “The lack of a diurnal variation of CH₄ EC flux observed when the wind was from the pond in this study was similar to the lack of a diurnal variation of CH₄ EC flux at another tailings pond reported by Zhang et al. (2019).”

L263-265: How do medians correlate? Take into account my earlier comments about representativeness as well.

605 Response: According to the numbers in Table 1, the median of CH₄ gradient flux is 20% lower than median EC flux. Again, the EC fluxes and gradient fluxes cover exactly the same periods and were calculated using the exact same measurements.

L270-272: This is quite far taken conclusion. Based on the results here you can only say that EC fluxes were used to calculate K_c, which of course then correlates well with EC.

610 Response: The idea behind this statement is that the K_c calculated in this way lets us calculate gradient fluxes for any species emanating from the pond that obeys the same physics (turbulent transport) and chemistry (inertness) as CH₄. Most gradient methods (modified Bowen, aerodynamic etc.) depend on some input of an EC flux, for example through u_∗ or the sensible heat, so there will always be some measure of autocorrelation. In our case, the link to the EC fluxes of methane are strictly through the parameterization of the Schmidt number, so a perfect correlation is not a given.

615 L272-274: And what were the outcomes of these studies? How do they compare to this study?

620 **Response:** These sentences were to show to compare our findings to the surprisingly few previous studies which compared EC flux and gradient flux of CH₄: “Zhao et al. (2019) compared CH₄ fluxes from an MBR method as well as from an aerodynamic flux model to EC fluxes for two small fish ponds, and showed that the MBR fluxes were well correlated with EC fluxes, with a mean 27% greater than the EC mean flux.” Such studies are rare, so we feel our contribution represents a useful addition to the body of studies investigating EC, eddy diffusivity, and gradient fluxes.

625 L278-281: Medians are actually not that different and means are within confidence intervals. Perhaps different time periods were used to calculate the averages of the two Sc's?

630 **Response:** The average of two Sc methods used exactly the same set of half-hour periods, which are the entire period of this campaign. With stability z/L corrected Sc, the mean gradient flux is closer to mean EC flux, compared to using the constant Sc.

635 L292: Above it is mentioned that the footprints are similar but here that they are different? How would the different footprint of the concentration measurement influence the flux?

640 **Response:** For infinite homogeneous upwind fetches, the methods have the same footprint, given correctly placed gradient levels. In real-life situations, there can be differences, since the upper gradient point has a larger concentration footprint than the lower one, and therefore may see sources farther upwind.

640 L297: “Results of IDM fluxes..”

Response: Fixed.

645 L297-298: Where is this shown?

Response: It is shown in another AMTD manuscript: <https://amt.copernicus.org/preprints/amt-2020-257>

650 L300: What are bubbling zones and where are they located? It comes as a surprise here that the chambers are not measured on the footprint of EC. If you measure bubbling zones with lots of ebullition, how is the chamber flux calculated? Don't the bubbles bring sudden bursts of methane, invalidating the normal flux calculation methods?

655 **Response:** The locations of the 15 flux chamber measurements are marked in the revised Figure 1. As can be seen, most of them fall within the EC footprint. It is possible that the sudden bursts of CH₄ could invalidate the flux chamber calculation and lead to an underestimation of flux, as discussed in Zhang et al. (2019). We wrote this in line 334-337. Integrated over the footprint of micrometeorological flux measurements, the intermittent nature of ebullition will have a minimal effect.

L300-305: How are large the medians compared to average fluxes?

660 **Response:** The median of the 15 measurements is 2.3 g m⁻²day⁻¹, and the mean is 2.8 g m⁻²day⁻¹. In addition, the 15 measurement fluxes were scattered indicating “the pond was highly heterogeneous in terms of CH₄ emissions”.

L332: replace “a month” with “five weeks”

665 **Response:** Fixed.

L336: Lower than what?

Response: Lower than results from three micrometeorological methods. Fixed.

670 L344: These are not comparable if not taken from same time periods and same footprints

Response: As explained in our response in the General Comments section above, the comparison between the chamber and micrometeorological flux measurements requires the assumption that emission rates from the pond did

675 not change much in the few days before, during and after the chamber sampling. This assumption is supported by
our CH₄ flux time series. We included this comparison to put results of this study into context of historical data and
current operational monitoring and reporting methods, and to shine the light on future monitoring needs, such as
seasonal variability of tailings pond emissions. We acknowledge in the text that “This reflects a general
680 complication when comparing the five weeks emission results in this study to annual emissions reported in the past.”

L365: Excactly, different time periods are compared with each other making the method comparison useless in this
form.

Response: Please see the response to the previous comment.

685 L383-386: In the equation there should be FCO₂ and FCH₄ instead of CO₂ and CH₄? These are results rather than
conclusions. Abbreviation CO₂eq is not defined and there are too many significant numbers in the result.

Response: Fixed.

690 Reference list: Two references are not peer reviewed yet, and there are quite many non-peer reviewed reports
included.

695 **Response:** It is an unfortunate reality that there is very little information in the peer-reviewed literature on industrial
fugitive emissions to the atmosphere in the Alberta Oil Sands, which is one reason for the importance of this current
manuscript. This lack of published information makes it difficult to avoid referring to grey literature. We have
removed the two references to the yet unpublished manuscripts by Moussa et al., and updated the information on the
You et al. manuscript on FTIR measurements in AMTD.

700 **References**

Fan, S. M., Wofsy, S. C., Bakwin, P. S., Jacob, D. J. and Fitzjarrald, D. R.: Atmosphere-biosphere exchange of CO₂
and O₃ in the Central Amazon Forest. *Journal of Geophysical Research*, 95: 16851-16864, 1990.

705 Mauder, M., and Foken, T.: Documentation and instruction manual of the eddy covariance software package TK2,
<https://core.ac.uk/download/pdf/33806389.pdf>, 2004.

Mauder, M., Liebethan, C., Göckede, M., Leps, J-P, Beyrich, F., and Foken, T.: Processing and quality control of
flux data during LITFASS-2003, Bound-Lay. Meteorol., 121, 67-88, 2006.

710 Moncrieff, J. B., Massheder, J. M., de Bruin, H., Ellbers, J., Friborg, T., Heusinkveld, B., Kabat, P., Scott, S.,
Soegaard, H., and Verhoef, A.: A system to measure surface fluxes of momentum, sensible heat, water vapor and
carbon dioxide, *Journal of Hydrology*, 188-189, page 589-611, 1997.

715 Sanches, L. F., Guenet, B., Marinho, C. C., Barros, N., and de Assis Esteves, F.: Global regulation of methane
emission from natural lakes. *Scientific Reports*, 9, (1), 255, 2019.

720

Methane emissions from an oil sands tailings pond: A quantitative comparison of fluxes derived by different methods

Yuan You^{1,§}, Ralf M. Staebler¹, Samar G. Moussa¹, James Beck², Richard L. Mittermeier¹

¹Air Quality Research Division, Environment and Climate Change Canada (ECCC), Toronto, M3H 5T4, Canada

²Suncor Energy Inc., Calgary, T2P 3Y7, Canada

[§]Now at Department of Physics, University of Toronto, Toronto, M5S 1A7, Canada

Correspondence: Ralf M. Staebler (ralf.staebler@canada.ca)

Abstract. Tailings ponds in the Alberta Oil Sands Region are significant sources of fugitive emissions of methane to the atmosphere, but detailed knowledge on spatial and temporal variabilities is lacking due to limitations of the methods deployed under current regulatory compliance monitoring programs. To develop more robust and representative methods for quantifying these emissions, three micrometeorological flux methods ([eddy covariance](#), [gradient](#), and [inverse dispersion](#)) were applied along with traditional flux chambers to determine fluxes over a 5-week period. Eddy covariance flux measurements provided the benchmark. A method is presented to directly calculate stability-corrected eddy diffusivities that can be applied to vertical gas profiles for gradient flux estimation. Gradient fluxes were shown to agree with eddy covariance within 7%, and inverse dispersion model fluxes within 11%, with an overall uncertainty of 28% for the calculated mean flux. Fluxes were shown to have only a minor diurnal cycle (18% variability) and to be mostly independent of wind speed, air and water surface temperatures. Flux chambers underestimated the fluxes by a factor of 2 in this particular campaign. These measurements indicate that the larger footprint of micrometeorological measurements results in more robust emission estimates representing the whole pond.

1 Introduction

Fossil fuel deposits in the Alberta Oil Sands Region consist of a mixture of quartz sands, silt, clay, bitumen, organics, trace metals, minerals, trapped gases, and pore water (Small et al., 2015). Surface mining is widely practised to extract the oil sands where the deposits are shallow. Extraction of the bitumen from the oil sands involves large amounts of warm water, various additives such as caustic soda and sodium citrate, and diluents, such as naphtha or paraffin (Simpson et al., 2010; Small et al., 2015). Non-recovered diluents, additives, and bitumen, along with water end up in large engineered tailings ponds.

There have been a number of studies to quantify the emissions of pollutants to the atmosphere from the various industrial activities associated with the Oil Sands (Simpson et al., 2010; Liggio et al., 2016; Li et al., 2017; Liggio et al., 2017; Baray et al., 2018; Liggio et al., 2019). Pollutant emissions that have been observed from tailings ponds include greenhouse gases (GHGs, mainly methane (CH₄) and carbon dioxide (CO₂)), reduced sulphur compounds, volatile organic compounds (VOCs), and polycyclic aromatic hydrocarbons (PAHs) (Siddique et al., 2007; Simpson et al., 2010; Yeh et al., 2010; Siddique et al., 2011; Siddique et al., 2012; Galarneau et al. 2014; Small et al., 2015; Bari and Kindzierski, 2018; Zhang et al., 2019). However, published studies on atmospheric emissions from tailings

Deleted: (AOSR)

Deleted: O

Deleted: S

ponds have been rare (Galarneau et al., 2014; Small et al. 2015; Zhang et al. 2019), and significant gaps remain regarding their contribution to total emission from oil sands operations (Small et al., 2015).

40 Quantifying greenhouse gases emissions from tailings pond is essential, since facilities are required to report specified gas emissions (Government of Alberta, 2019) and to follow emission standards (Statutes of Alberta, 2016). CH₄ is long-lived in the atmosphere and has a greenhouse gas warming potential per molecule that is 28 times that of CO₂ on a 100-year time horizon, contributing 0.97 W m⁻² radiative forcing to the total of 2.83 W m⁻² by all well-mixed greenhouse gases since the beginning of the industrial era (Myhre et al., 2013). CH₄ can be produced by microbes in
45 the oil sands tailings through methanogenic degradation of hydrocarbon in diluents and unrecovered bitumen (Siddique et al., 2007; Penner and Foght, 2010; Siddique et al., 2011; Siddique et al., 2012; Foght et al., 2017; Kong et al., 2019).

Most commonly, flux chambers have been used to determine emission rate of GHGs from tailings ponds (Small et al., 2015; Stantec, 2016). These chambers cover an area of less than 1 m² each and result in only short snapshots of
50 emissions that may not capture the spatiotemporal variability of emissions. Tailings ponds in the oil sands region typically have a size of 0.1-10 km² with heterogeneous surfaces. Micrometeorological methods of determining fluxes, such as eddy covariance (EC) (Foken et al., 2012) and gradient fluxes (Meyers et al., 1996), are non-intrusive and continuous methods that can be used to measure fluxes from area sources. These methods intrinsically produce integrated flux estimates representative of hectares to km². In addition, inverse dispersion models (IDMs) (Flesch et al., 1995) and vertical radial plume mapping (VRPM) (Hashmonay et al., 2001) can be used to combine
55 micrometeorological information with measured pollutant concentrations to deduce emission fluxes.

Micrometeorological methods applied to large areas of a tailings pond can provide much needed information on the spatial and temporal variabilities of emission fluxes from tailings ponds as an input for air quality and climate change modelling. Tailings ponds represent a useful testing ground for a multi-method comparison of flux measurement
60 techniques due to their reliability as sources of significant fluxes that are relatively well-defined spatially. This manuscript describes the results of a study comparing flux chambers, eddy covariance, gradient and IDM approaches for estimating emission rates, using a variety of instruments.

2 Site and measurement description

The main site of this study was on the south shore of Suncor Pond 2/3 (Fig. 1; 56°59'0.90"N, 111°30'30.30"W, 305m
65 ASL). The Suncor main facility was 2.6 km to the northeast, and the Syncrude main facility 9 km to the northwest.

The pond liquid surface area was about 2.5 km by 1.3 km. Within 2 km to the south of our measurement site, the landscape included natural landscapes, a workers camp, and parking lots. There were also other facilities and sources
70 around the pond, but too far from our measurement site to contribute to the fluxes measured using the methods in this study (Section 4.2). Measurements were conducted from July 28 to September 5, 2017. The sampling platform was a 32 m mobile tower instrumented at three levels (8m, 18m, and 32m) above ground, plus another sampling level at 4 m above ground on the roof of the trailer housing the instruments. This setup allowed the measurement of the vertical gradient of gaseous pollutants concentrations and meteorological conditions. Gas inlets at these levels were connected to a range of instruments in the trailer located right beside the flux tower, through 45 m of ½" (1.27 cm) Teflon tubing

Deleted: Field Study

Deleted: trees,

for the upper three levels and 7 m of tubing for the lowest level. A cavity ring-down spectroscopy (CRDS) instrument (Picarro, Model G2311f) was used to measure the mole fraction of CH₄, CO₂ and H₂O at 10Hz. It sampled from the 18m level through a 30 m 3/8" outer diameter Teflon tube at a flow rate of 7 L min⁻¹, ensuring turbulent plug flow.

For the gradient measurements, a cavity ring-down spectroscopy instrument (Picarro, Model G2204) was used to measure CH₄ and hydrogen sulfide (H₂S) at four levels by cycling through the levels every 10 minutes (i.e. 2.5 minutes at each level). Readings from the first 30 s after each level switch were discarded. Calibrations of CH₄ for all the CRDS instruments were performed before and after the field project against secondary standards traceable to standards used by Environment and Climate Change Canada (ECCC) for their GHG Observational Program, which are in turn traceable to World Meteorological Organization (WMO) standards.

At each of the three levels on the tower, an ultrasonic anemometer (Campbell Scientific, Model CSAT3) measured the turbulent motions in the atmosphere, i.e. u, v, w (the three orthogonal components of the wind) and T (sonic temperature), at 10Hz. The momentum flux and the sensible heat flux can be calculated from the covariance of the vertical wind component with horizontal wind and temperature fluctuations respectively through eddy covariance. Friction velocity (u_*) can also be calculated from measured u, v, and w. The two lower ultrasonic anemometers pointed towards true north, whereas the ultrasonic anemometer at 32 m pointed at 3.5°. An adjustment to the true north was applied during analysis. There was also a propeller anemometer (Campbell, Model 05103-10) on the trailer roof 4 m above ground, measuring wind speed and direction. Ambient temperature and relative humidity (RH) were measured with sensors at three levels on the tower and 1m above ground (Rotronic, Model HC2-S3-L; shield: Campbell Scientific, Model 43502). Ambient pressure was measured with a barometer (RM Young Model 61202). A net radiometer (Kipp & Zonen, Model CNR1) was used to measure solar radiation during the entire project. An infrared remote sensor (Campbell Scientific, Model SI-111) was mounted at 32m on the tower looking down at an angle of 30° below horizontal to measure the temperature at the pond surface. With an angular field of view of 44°, this results in a footprint ranging from 25 m to 228 m from the tower. Given the location of the tower relative to the pond, winds from between 286° and 76° were defined as coming from the pond.

An open-path Fourier transform infrared (OP-FTIR) spectrometer system (Open Path Air Monitoring System (OPS), Bruker) was set up at the site to measure line-integrated mole fractions of CH₄ and other pollutants. The spectrometer was set up in a trailer next to the main tower about 1.7 m above the ground, pointing to three retro-reflectors 200 m to the east. The lowest retro-reflector was on a tripod, and the higher two retro-reflectors were supported by JLG basket lifts, resulting in heights of the three retro-reflectors of approximately 1.7 m, 11 m, and 23 m above ground. The spectrometer automatically cycled through pointing at these three sequentially. Spectra were measured at a resolution of 0.5 cm⁻¹ with 250 scans co-added, resulting in roughly one-minute resolution. Other details on the OP-FTIR setup and spectral retrieval analysis can be found in You et al. (2020).

Deleted: 4

Deleted: A

Deleted: three

Deleted: .

Deleted: and a CRDS instrument (Picarro, Model G2401-M) was used to measure CH₄, CO₂, CO and H₂O at four levels

3 Methods for deriving fluxes

115 3.1 Eddy covariance flux

Eddy covariance (EC) fluxes represent a direct measurement of the turbulent vertical exchange of a substance, and as such usually serves as a [reference](#) (Foken et al., 2012) to which more indirect methods (such as those described below) can be compared (Bolinius et al., 2016; Prajapati and Santos, 2018). Eddy covariance typically requires fast response time measurements ([on the order of 0.1 seconds](#)) and [high sampling frequency \(> 5Hz\)](#). (Foken et al., 2012), which in 120 this study limits the method to sensible and latent heat (H₂O) fluxes, momentum, CO₂ and CH₄ [fluxes](#).

As summarized in Foken et al. (2012), [the eddy covariance method](#) simply calculates the flux by averaging the product of the deviations of the vertical wind component and a mole fraction from the mean. For compound *c* and vertical wind component *w*, the flux F_c is thus

$$F_c(EC) = \overline{w'c'} \quad (1)$$

125 where the mole fraction $c = \bar{c} + c'$, with the overbar denoting the average and the prime a deviation from it, and similarly for *w*. [To account for “storage”, i.e. the vertical build-up or venting of a gas between the source and the measurement level, a storage term is added, so that the total flux is given by](#)

$$F_c = \overline{w'c'} + \int_0^z \frac{\partial c}{\partial t} \partial z \quad (2)$$

In this study, 30-min averages of the EC flux of CH₄ were calculated by combining the 18 m CRDS CH₄ data with 130 the CSAT measurements. The raw data were processed by Eddypro (version 6.0.0, LI-COR Inc.), and major processes included axis rotation ([double rotation](#)) (cf. [Wilczak, et al., 2001](#)), time lag compensation ([covariance maximization method](#)) ([Fan, et al., 1990](#)), and storage term correction (Foken et al., 2012). The EC flux quality flag was [categorized into 3 classes](#): 0 (best quality), 1 (good quality), and 2 (poor quality) (Mauder et al., 2006; [Mauder and Foken, 2004](#)). EC fluxes with flag 0 and 1 were included in further analysis.

135 3.2 [Gradient flux method](#)

Gradient flux estimates are based on relationships between the vertical gradient of mole fractions and the associated flux (down the gradient from high to low mole fractions). In the atmosphere, turbulent exchange dominates molecular diffusion by several orders of magnitude under most conditions, and the factor relating the gradient to the flux is a transfer coefficient dependent on the characteristics of turbulence (first-order closure, *K*-theory), called the eddy 140 diffusivity (K_c) (Stull, 2003a). The flux is then given by

$$F_c = -K_c \frac{\partial c}{\partial z} \quad (3)$$

Where F_c is the gradient flux for a pollutant *c*, and $\frac{\partial c}{\partial z}$ is the vertical mole fraction gradient. Note that in this notation, K_c incorporates any stability corrections required since stability effects on the relationship between vertical mole fraction gradients and turbulent fluxes are already incorporated. Our approach follows the well-established “modified 145 Bowen Ratio” (MBR) method (Meyers et al., 1996; Bolinius et al., 2016). To calculate K_c of CH₄, the measurements

Deleted: the benchmark

Deleted: > 5 Hz

Deleted: To capture the full spectrum or relevant eddy sizes, measurements need to typically be done at > 5 Hz (for the smallest eddies), and the average needs to be 15 minutes or more (to capture the largest eddies).

Deleted: WPL (Webb-Pearman-Leuning) density correction,

Deleted: in three categories

Deleted:)

Deleted: Flux vertical gradient

of CH₄ EC flux and a gradient of mole fraction are required by Eq. (3). From the measurements at the 18 m, we have a direct EC flux for CH₄. Since the footprint of fluxes derived from mole fraction gradients between 8 m and 32 m is approximately equivalent to the EC footprint at 18 m (see discussion in Section 4.2), this gradient can be combined with the EC flux to calculate K_c by Eq. (3). However, only a fraction of the observations yield well-resolved CH₄ fluxes and gradients, whereas a continuous time series of K_m , the eddy diffusivity for momentum (wind speed) by Eq. (4) (Stull, 2003a), can be readily established. Therefore, we establish a relationship between K_c and K_m for those periods when this is feasible, and calculate the ratio of these two, which by definition is the so-called “Schmidt Number” in Eq. (5) (Gualtieri et al. 2017),

$$F_m = -K_m \frac{\partial u}{\partial z} \quad (4)$$

$$S_c = \frac{K_m}{K_c} \quad (5)$$

A near-continuous time series of K_c is then calculated from Eq. (5) and applied to the mole fraction gradients for all the gases measured on the gas profile system to calculate fluxes.

To get the Schmidt Number S_c by Eq. (5), two approaches were used: the first approach is with a constant S_c . Measured K_c was binned with and plotted against K_m . The linear regression of binned K_c with K_m bins was performed. The inverse of this slope (Fig. 2), as defined in Eq. (5), is the Schmidt Number. The least-squared fit produces a $S_c = 0.923$, which compares to published values of 0.99 (Gualtieri et al., 2017). Since due to the intermittent nature of CH₄ a measured K_c is only available a fraction of the time, we use the more continuous momentum eddy diffusivity K_m divided by S_c as our K_c .

The second approach is with variable S_c . Gualtieri et al.(2017) reviewed experimental and numerical simulation studies of turbulent Schmidt number in the atmospheric environment, and reported S_c values from 0.1 to 1.3. Flesch et al. (2002) measured turbulent S_c of a pesticide in the atmosphere from soil emissions. Reported S_c in that study varied from 0.17 to 1.34 and showed that this was not solely due to measurement uncertainty. The S_c in this study also varies significantly over time when the wind was from the pond, from 0.04 to 3.26.

To investigate the real variability in S_c , $S_c = K_{m_measured}/K_{c_measured}$ was plotted against the stability parameter z/L (Stull, 2003b), where L is the Obukhov length, for periods when the wind was from the pond direction (Fig. 3). Figure 3 shows that S_c becomes small as z/L indicates increasingly unstable turbulent mixing, i.e. an increasing importance of convective (sensible heat driven) turbulence, which is not captured by an uncorrected K_m , vs. mechanical (momentum driven) turbulence. S_c varies significantly with z/L , and is associated with significant noise near neutral stability (z/L close to 0). To avoid introducing large scatter in the S_c correction near neutral stability, S_c is set as 0.923 when z/L is close to 0. To make the correction function continuous, a step-wise definition for S_c is given:

$$S_c = \begin{cases} 0.126 + 7.81 \times 10^{-9} e^{\left(\frac{z}{L} + 19.5}{1.039}\right)}, & \frac{z}{L} < -0.34 \\ 0.923, & \frac{z}{L} \geq -0.34 \end{cases} \quad (6)$$

This S_c of the entire study period and a time series of $K_c = K_m/S_c$ (corresponding to 8m and 32m measurements) were calculated. Then the gradient flux of CH₄ with corrected K_c was calculated by Eq. (3). Negative half-hour CH₄ gradient fluxes have been filtered out when the EC flux was positive during the same half-hour, since they are most likely due

190 to problems such as shifting wind directions, and unsuitable for calculating gradient fluxes. In the Results and
Discussion section, gradient fluxes and plots from the variable S_c approach are shown, and results with constant S_c
approach are shown in Table S1 for comparison.

3.3 Inverse dispersion fluxes

195 Inverse dispersion models (IDMs) can be used to derive emission rates estimates based on line-integrated or point
mole fraction measurements downwind of a defined source. Required inputs include the turbulence statistics between
the source and point of observation. Unlike the EC and gradient techniques, IDMs also require an estimation of the
background mole fraction of the pollutant upwind of the source. The backward Lagrangian Stochastic (bLS) models
are a specific subtype of IDMs. WindTrax 2.0 (Thunder Beach Scientific, <http://www.thunderbeachscientific.com>
(Flesch et al., 1995)) based on a bLS model, is used in this study. The emission rate is calculated through:

$$200 \quad Q = \frac{(C - C_b)}{\left(\frac{C}{Q}\right)_{sim}} \quad (7)$$

where C is the pollutant concentration at the measurement location, C_b is the background mole fraction of the pollutant,
and $(C/Q)_{sim}$ is the simulated ratio of the pollutant mole fraction at the site to the emission rate from the specified
source calculated by the bLS model. In this study, the meteorological condition inputs for bLS model are u^* and L
taken from the 30-min averaging calculation of ultrasonic anemometer measurements at 8 m, as well as 30-min
205 average wind directions and ambient temperature directly from the propeller and temperature sensor at 4 m. Periods
when $u^* < 0.15$ m/s were disregarded (Flesch et al., 2004). CH_4 mole fraction input was taken from the OP-FTIR
measurement which was located 10m to the east of the flux tower. Emission rates are calculated by IDM only when
the wind came from the pond, including the sectors centred at 270° and 90° .

Deleted: right beside

Deleted: on the east

3.4 Flux chamber measurements

210 Floating flux chamber measurements of CH_4 and CO_2 were conducted at 15 spots, including 4 within 500 m of the
tower, from Aug 31 to September 2, 2017, by Barr Engineering Co., using compliance monitoring procedures
established with guidance from the *Quantification of Area Fugitive Emissions at Oil Sands* issued by Alberta
Environment and Parks (AEP 2014). On-site analysis of GHG was performed using U.S. Environmental Protection
Agency (USEPA) flux chambers with real-time GHG analyzers (Los Gatos Research, Inc., USA). These flux chamber
215 measurements were conducted during daytime. Key procedural steps include, 45 minutes of purging pure nitrogen gas
to reach an equilibrium between the flow of the inert carrier gas and the methane evolving from the pond surface, and
measurement for a minimum of 30 minutes of steady-state concentration. Fluxes were calculated according to the
USEPA users guide EPA/600/8-86/008 (AEP 2014). GHG gases reported from the chamber measurements include
 CH_4 , CO_2 and N_2O .

Deleted:

Deleted: with sample durations

Deleted:

Deleted: ranging from 74 to 116 minutes, most of which was for the stabilization of the gas flow inside the flux chamber (i.e. to reach an equilibrium between the flow of the inert carrier gas and the methane evolving from the pond surface)

220 3.5 Area weight-average of flux

To derive fluxes representing the whole pond, the half-hour fluxes are binned by wind direction into 16 sectors.
Area weighted averages of fluxes for the pond F_{pond} are then calculated by

$$F_{pond} = \frac{\sum_{sectors} \overline{F(flux,sector)} \cdot Area(sector)}{\sum_{sectors} Area(sector)} \quad (10)$$

4 Results and Discussion

4.1 Meteorological conditions

235 Given the setup of this study at this pond (Fig. 1), the wind coming from the north (wind direction (WD) $\geq 286^\circ$ or
 WD $\leq 76^\circ$) was considered as wind from the pond direction. As shown in the wind rose (Fig. S1), wind coming from
 the pond occurred only about 22% of the entire measurement period. The dominance of winds from the background
 directions was known before the study, based on records from monitoring stations in the area, but logistical and access
 constraints limited us to using the south shore for the setup. There was no significant diurnal variation in wind direction
 240 over the entire period. The ambient temperature during the measurement period varied from 7.5 to 31.1 °C, with an
 average of 17.5 °C (Fig. 4(b)). The mean wind speed measured with the propeller anemometer at 4 m was 3.0 m s⁻¹,
 with a range from 0 to 14.9 m s⁻¹ and quartiles of 1.7 and 4.0 m s⁻¹ (Fig. 4(a)). The mean friction velocity at 8 m (the
 lowest height by sonic anemometer measurement) over the whole measurement period was 0.32 m s⁻¹ (Fig. 4(a)), with
 a range from 0.03 to 1.01 m s⁻¹ and quartiles are 0.20 and 0.42 m s⁻¹. Wind speed and friction velocity had a predictable
 245 diurnal pattern, greater during the day than at night (Fig. 4(a)).

In Fort McMurray during the study period, the sunrise was in the range of 4:35 to 5:56 MDT (Mountain Daylight
 Savings Time, UTC-6), solar noon occurs at around 13:30 and sunset occurs in the range of 22:25 to 20:49 MDT (Fig.
 4(d)). Winds across the pond and from the south pass over markedly different surface types (liquid pond vs. a mixture
 of solid surface types), so the sensible heat flux H is analyzed separately based on the wind direction (Fig. 4(e)).
 250 During the day (from 8:00 to 19:00), H associated with winds across the pond was consistently smaller than H with
 winds from other directions, suggesting the pond absorbs significant solar energy at the site during the day. It is also
 worth mentioning that H stayed positive during the night when the wind came across the pond, consistent with the
 observation that the pond surface temperature was greater than the air temperature (Fig. 4(c)). These resulted in
 convective turbulent transport of species emitted from the pond surface throughout the night.

4.2 Footprint of flux measurements

The footprint of a micrometeorological flux measurement, i.e. the area upwind that contributes to the flux at the point
 of observation, depends on the wind speed and the dynamic stability of the surface layer. The footprints of EC fluxes
 measured at 18m at each half-hour period were estimated using the algorithm by Kljun et al. (2015), which takes mean
 wind speed, boundary layer height, wind direction, friction velocity, Obukhov length, and standard deviation of
 260 horizontal wind speed. Boundary layer height was estimated using the LIDAR measurements at Fort McKay in August
 2017 (Strawbridge et al., 2018). Footprints under unstable conditions are summarized in the polar plot in Fig. 1.
 Footprint contribution distances were calculated for each half-hour over the entire period of study. Results were further
 separated into unstable ($z/L < -0.0625$), neutral ($-0.0625 < z/L < 0.0625$), and stable ($z/L > 0.0625$) conditions. Since
 unstable conditions took 98.6% of time when the wind was from the pond and 52% of entire measurement period, we

Deleted: ame

Deleted:

Deleted: (Fig. S2)

Deleted: during mid-August

Deleted: is near 6:00

Deleted: around

Deleted: 21:00

Deleted: b

Deleted: 2013

Deleted: An example of the footprint is shown in Fig. S3 (a), and

Deleted: f

Deleted: over the entire measurement period

Deleted: rose

Deleted: S3 (b)

280 summarized the unstable conditions footprint results into 16 wind direction bins, and medians are shown in the polar
plot in Fig.1. The footprint results show the EC flux footprint lies mostly within the edges of the pond.
For gradient flux measurements, the effective footprint is the same as the EC footprint at the geometric mean of the
two sample heights (Horst, 1999), for a homogeneous surface area upwind. In this study, gradients between 8 m and
32 m therefore have a footprint equivalent to that for EC at 16 m, reasonably close to where the 18 m EC fluxes were
measured. Since the concentration footprint at the upper (32 m) level is larger than the concentration footprint at the
285 lower (8 m) level, the gradient flux may be affected by sources beyond the geometric mean footprint.

Deleted: showing
Deleted: under most conditions
Deleted: flux gradient
Deleted: however

4.3 Eddy covariance flux

Analysis of CH₄ mole fractions at 18 m as shown in Fig. 5 clearly indicates that CH₄ was elevated when the wind was
from the pond direction, and it was steady at round 1.9 ppm when the wind was from other directions (Fig. 5 and 6).
Besides sectors from the pond directions, Fig. 7 shows CH₄ fluxes significantly larger than zero from two sectors
290 centred with 270° and 90°. These two sectors cover the boundaries of pond and non-pond areas. Therefore, measured
results for air coming from these two sectors could represent a mixture of air carrying pond emissions and air from
the southwest close to the pond shoreline. EC fluxes from the four wind directions sectors centred in the range of
292.5° to 0° are close to each other.

There was no discernible diurnal pattern of the CH₄ EC flux when the wind came from the pond direction (WD ≥
295 286°, or WD ≤ 76°) (relative standard deviation is 18%) (Fig. S2 (a)). Diurnal pattern of another three sectors when
the wind was not from the pond were studied. The sector 259° ≤ WD < 286° (Fig. S2 (b)) contains a mixture of pond
emission and the shore of pond, and it also showed no significant diurnal pattern. The sector 214° ≤ WD < 259°
(Fig. S2 (c) mainly covers trees and a lake, and showed a slightly increased flux during 12:00-18:00, which is likely
due to biogenic emission from trees and soils (Covey and Megonigal, 2019). The sector 124° ≤ WD < 146° (Fig. S2
300 (d)) covered a workers' lodge and parking lots, and CH₄ emissions and diurnal variation were close to zero. The lack
of a diurnal variation of CH₄ EC flux observed when the wind was from the pond in this study was similar to the lack
of diurnal variation of CH₄ EC flux at another tailings pond reported by Zhang et al. (2019).

Deleted: S4
Deleted: S4
Deleted: S4
Deleted: S4

Relationships between the flux and various meteorological parameters were investigated, and results show that fluxes
were independent of wind speed, u^* , water surface temperature, or the temperature difference between the water
surface and 8 m (Fig. S3), i.e. they were not drivers of the CH₄ emission rate. CH₄ at this site is mainly produced
305 through the methanogenesis of hydrocarbon by the microbes in the fine tailings covering a range of depth in the pond
(Penner and Foght, 2010; Siddique et al., 2011; Siddique et al., 2012), and therefore is not affected much by the
meteorological conditions at the surface or above the pond.

Deleted: S5

4.4 CH₄ gradient flux and comparison with EC flux

310 The CH₄ mole fraction measured at 8 m and 32 m show that winds across the pond carried significantly more CH₄
than from other directions, and there was a clear vertical gradient with mole fraction at 8 m on the order of 0.5 ppm
or more higher than at 32 m (Fig. 6). Gradient fluxes were calculated for all periods when valid EC fluxes and
concentration gradients were available. The gradient flux derived from measurements at 8m and 32m shows that the

flux was minimal when the wind was from other directions, similar to the EC flux (Fig. S4). The average CH₄ gradient flux was 7% less than the EC flux (Table 1), and CH₄ gradient flux agreed well with EC flux (slope=1.03, r²=0.65) (Fig. 8). All comparisons are based on the set of simultaneous half-hour periods when both EC and gradient fluxes were available.

Deleted: S6

Studies comparing MBR and eddy covariance CH₄ fluxes are rare. Zhao et al. (2019) compared CH₄ fluxes from an MBR method as well as from an aerodynamic flux model to EC fluxes for two small fish ponds, and showed that the MBR fluxes were well correlated with EC fluxes, with a mean 27% greater than the EC mean flux. The gradient flux calculation in our study can be considered a hybrid of the MBR and aerodynamic methods, based on a continuous time series of eddy diffusivities for momentum, scaled by the eddy diffusivity for CH₄. The gradient fluxes of CH₄ agree well with EC flux in our study, indicating that the derived eddy diffusivity K_c for CH₄ can be utilized for other gaseous pollutants when the wind was from the pond direction (Meyers et al., 1996). Gradient fluxes of VOCs and reduced sulfur components from the pond are discussed in Moussa et al. (2020a) and Moussa et al. (2020b). Other studies comparing MBR with eddy covariance methods on other gases fluxes, such as CO₂, have been reported. Xiao et al. (2014) showed that fluxes of CO₂ from these two methods were comparable at Lake Taihu. Wolf et al. (2008) and Bolinius et al. (2016) used eddy diffusivity of heat to derive gradient fluxes of CO₂ over trees, and showed they were comparable with EC fluxes.

Gradient fluxes were also calculated with the constant S_c approach, as described in Section 3.2, and results are listed in Table S1. Gradient flux calculated from a constant S_c were lower than gradient fluxes with the variable S_c approach. Results from this study clearly present the variable nature of S_c , and that correcting S_c with stability z/L is effective to improve gradient flux calculations. After correcting S_c , CH₄ gradient fluxes compared well with EC flux.

4.5 CH₄ inverse dispersion flux and comparison with EC flux

Compared to point measurements, path-integrated measurements have the advantage of being less sensitive to changes of wind direction and being representative of larger areal averages (Flesch et al. 2004). Therefore, the bottom path-integrated CH₄ mole fraction of the FTIR was used as input for IDM flux estimate. The bottom path measurement had the greatest signal-to-noise ratio, and a footprint of on the order of 1-2 km, which is comparable to the footprint of the EC and gradient fluxes (Fig. 4). CH₄ IDM flux calculated from the path-integrated mole fraction inputs from OP-FTIR bottom path measurements compared well to EC flux, based on the set of simultaneous half-hour periods when both EC and IDM fluxes were available. IDM and EC flux showed reasonable correlation (r²=0.46) with a slope of 0.93 (Fig. 9). The interquartile ranges of the fluxes from these two methods overlap. The average of result IDM flux was 11% smaller than EC flux. Consistent with EC flux, IDM flux also showed minimal diurnal variations when the wind came from the pond directions (Fig. S5), with smaller fluxes from 8:00 to 20:00. Some of the differences are likely due to the different footprints of the two measurements. The footprint for turbulent fluxes is smaller than the footprint for concentrations at the same height (Schmid, 1994).

Deleted: S3

Deleted: based on

Deleted: S7

Since the background mole fraction input for IDM calculation could affect the flux estimates, two approaches of determining background mole fraction of CH₄ for model inputs were tested: the daily minimum of CH₄ from wind sectors between 180° and 240° of OP-FTIR at our site; the CH₄ from another independent OP-FTIR measurement on the north

shore of this pond (details are described in You et al. (2020)). Results IDM fluxes with these two background approaches agreed well (You et al. 2020).

365 4.6 Flux chamber measurements

Fluxes from the 15 measurements over 3 days in the bubbling zones varied from 0.9 to 5.1 g m⁻² d⁻¹, with an average of 2.8 g m⁻² d⁻¹ and a median of 2.3 g m⁻² d⁻¹. The average flux of the five measurements on the last day Sept 2 is 3.6 g m⁻² d⁻¹, which is the highest amongst the 3 days. The great variation amongst these 15 measurements show the pond was highly heterogeneous in terms of CH₄ emissions. The average fluxes from these flux chamber measurements are about half of average fluxes from EC, gradient, and IDM methods. While the flux chamber measurements were deployed over the three days, the wind was from the south, so no simultaneous comparison could be made between flux chamber measurements and micrometeorological methods. However, based on the micrometeorological fluxes spanning more than a month, there is no evidence of day-to-day variability of this magnitude, and we conclude that the mismatch is due to spatial or methodological differences.

370 Annual compliance flux chamber measurements in 2016 resulted in pond average fluxes of 5.3 g m⁻² d⁻¹, and 11.1 g m⁻² d⁻¹ in 2018, despite similar operational parameters in these years as in 2017. We conclude that the underestimate in 2017 is not an indication of a systematic bias of flux chambers, but rather a measure of the uncertainty involved in flux estimates based on snapshot chamber measurements.

A few other studies have also discussed differences between flux chambers and micrometeorological methods. Zhang et al. (2019) measured CH₄ emission from another tailings pond, and reported flux chamber measurements were more than 10 times greater than fluxes from EC method. They stated that strong eruptions of bubbles could overwhelm the chamber to result in a local underestimation of the flux. On the other hand, the lower EC flux estimate suggests that the area average flux was being overestimated by extrapolation from the chambers, which may have preferentially been located over bubble zones. Their EC fluxes were two orders of magnitude smaller than CH₄ flux in this study. Results from this study and Zhang et al. (2019) suggest that average tailings pond CH₄ emission extrapolated from a few individual flux chamber measurements may significantly underestimate or overestimate fluxes relative to area-averaging micrometeorological measurements.

This has also been shown over other water surfaces. Podgrajsek et al. (2014) investigated CH₄ fluxes at the lake Tammaren, and reported the fluxes from EC and flux chamber were on the same order of magnitude. They stated due to the non-continuous measurement of flux chambers, some high flux short episodes could be missed. Schubert et al. (2012) measured CH₄ fluxes from Lake Rotsee, and reported the fluxes from EC and flux chamber compared well. Erkkilä et al. (2018) measured CH₄ flux at Lake Kuivajärvi with the two methods when the lake was stratified, and reported flux chamber measurements were significantly greater than EC fluxes. In conclusion, due to the spatial heterogeneity of fluxes on a scale smaller than the spatially integrating micrometeorological methods, reliance on a limited number of flux chamber measurements can result in significant year-to-year variability.

Deleted:

4.7 Comparison with previous results

Emissions reported in Small et al. (2015) and a Stantec report (2016) (Table 2) represent estimates extrapolated from individual flux chamber measurements, and did not incorporate any seasonal variations for microbial CH₄ emissions.

400 Therefore, to compare result of this study to results summarized in Small et al. (2015), we simply used 1 year =365 equal days. Small et al. (2015) showed that CH₄ emissions from the same pond were 2.6 g m⁻² d⁻¹ based on the averaging of flux chamber measurements during August to October in 2010 and 2011. A Stantec compliance report (2016) presented flux chamber measurements on this pond with resulting average fluxes of 12.9 and 2.1 g m⁻² d⁻¹ (bubbling and quiescent zones, respectively) in 2013, and 9.6 g m⁻² d⁻¹ and below detection limit respectively in 2014.

405 Eddy covariance fluxes of CH₄ in this study are 120% greater than flux chamber measurements which were taken during the last few days of this project and 134% greater than emissions reported in Small et al. (2015). However, CH₄ fluxes in this study are 36% to 52% smaller than the fluxes from the bubbling zones in 2013 and 2014 (Stantec, 2016). The big differences between flux chamber measurements in the bubbling and quiescent zones may suggest micrometeorological measurements with a bigger footprint will perform better in quantifying emission from the whole

410 pond. It is worth noting that the seasonal variation of fugitive emission from tailings pond is still not well understood, and that different daily emissions are derived from the tabulated annual results from Small et al. (2015) depending on the annual extrapolation model used. This reflects a general complication when comparing the five weeks emission results in this study to annual emissions reported in the past.

Baray et al. (2018) calculated CH₄ emission from this pond based on airborne measurement in 2013 over the whole facility, combined with reported statistics stating that 58% of CH₄ emissions within the facility were from tailings ponds, and 85% of emissions from these tailings ponds were from Pond 2/3. This resulted in an estimate of 2.0 ± 0.3 tonnes h⁻¹, which converts to 17.1 g m⁻² d⁻¹ (for a pond area of 2.8 km², Small et al. (2015) Table 2). This emission rate is significantly (180%) greater than emissions from the three micrometeorological methods in this study, possibly because of the uncertainties in the reported percentage contribution of CH₄ emissions from this pond to the whole

420 facility.

Suncor reported facility-wide emissions of CH₄ for 2017 of 5977 tonnes (Government of Canada, 2017). The emissions measured during the 5 weeks of this study extrapolated to the year result in 5121 tonnes yr⁻¹, i.e. 86% of this total. This extrapolation assumes seasonal invariance of CH₄ emissions (e.g. January emissions are the same as August emissions) as is common practice in monitoring reports (cf. Stantec, 2016).

425 When comparing CH₄ emissions in this study to emissions summarized in Table 2, it must be kept in mind that different time periods are being compared, and that several factors may contribute to variability of the emissions (Siddique et al. 2007 and 2012). Pond 2/3 is an active pond, and the amount and characteristics of input streams are variable with time. Some of the facility specific variables which could affect the methane emissions include: the amount of diluent loss to the pond, the proportions of diluent and hydrocarbons in the froth treatment tailings (FTT) that enter matured fine tailings (MFT) layers in the pond, density of microbes in the MFT, physical disturbance of

430 the MFT layers, transferring activities of the MFT, pond water temperature change and consequential density inversion

Deleted: Results in this study have provided several estimates of the emission of CH₄ from this tailings pond using different micrometeorological methods, for a period of a month. The gradient and inverse dispersion methods agreed well with the more fundamental eddy covariance results (within 7% and 11%), which lends confidence that the former two methods can reliably provide flux estimates for other gases emanating from the pond. These results were also compared to flux chamber measurements at this pond taken during the study, showing flux chamber estimates were 54% lower in 2017. ¶

Deleted:

Deleted: 1

445 between oil layers and water in the pond, FTT discharge diluent composition change, introduction of new materials
and chemicals into the MFT, and consequential change in microbial community (Small et al. 2015; Foght et al. 2017).
Another independent approach of estimating CH₄ emissions is using an emission factor (EF) combined with diluent
discharge rates to the pond. The EF was based on an MFT characterization and kinetics of methanogenesis for a
matured pond. Pond 2/3 is presumably similar in maturity and properties with the studied MFT in other oil sands
facility (Siddique et al. 2008). After incorporating the diluent loss to the pond, the daily CH₄ emissions were calculated
450 and integrated into an annual emission of 5860 tonnes for 2017, comparable to annual emissions extrapolated from
the micrometeorological methods in this study. This approach requires some assumptions: first, that the kinetics of
methanogenesis are a function of the maturity of the microbial community within the target MFT; and second, that
the properties of the diluent feed stream remain constant over the period considered. This approach can provide
emission estimates continually provided that the microbial state in the MFT and the diluent discharge volumes and
455 properties are tracked and remain consistent.

To put the CH₄ emissions into a global warming context, the CH₄ fluxes can be combined with concurrent flux
measurements of CO₂ with the same instrumentation. Assuming a global warming potential (GWP) of CH₄ = 28
(Myhre et al., 2013), the equivalent CO₂ flux from this tailings pond $F_{CO_{2eq}} = F_{CO_2} + (F_{CH_4} \times GWP) = 159$ kilo
tonnes year⁻¹. This accounts for only 2% of Suncor's facility CO_{2eq} emissions in 2017 due to the dominance of CO₂
460 emissions.

5. Conclusions

Results in this study have provided several estimates of the emission of CH₄ from this tailings pond using different
micrometeorological methods, for a period of five weeks. The gradient and inverse dispersion methods agreed well
with eddy covariance results (within 7% and 11%), which lends confidence that the former two methods can reliably
465 provide flux estimates for other gases emanating from the pond. These results were also compared to flux chamber
measurements at this pond taken during the study, showing flux chamber estimates were 54% lower in 2017 than
those from micrometeorological methods. The good agreement between the three micrometeorological measurements
flux results indicate that the larger footprint of micrometeorological measurements results in more robust emission
estimates representing the whole pond.

In addition, fluxes were shown to have only a minor diurnal cycle, with an 18% variability, during the period of this
470 study. To investigate seasonal patterns, further studies will be required in the future.

Data availability.

All data are publically available at <http://data.ec.gc.ca/data/air/monitor/source-emissions-monitoring-oil-sands-region/emissions-from-tailings-ponds-to-the-atmosphere-oil-sands-region/>.

475 **Author contribution.**

YY and RS conducted the research and wrote the manuscript; SGM contributed flux analysis and editing; RM contributed CH₄ data; JB contributed operational data on the pond and contributed to the writing.

Competing interests.

Dr. Beck is an employee of Suncor Energy. The other authors have no competing interests.

480 **Acknowledgements.**

The authors thank the technical team of Andrew Sheppard, Roman Tiuliugenev, Raymon Atienza and Raj Santhaneswaran for their invaluable contributions throughout, Julie Narayan for spatial analysis, Stewart Cober for management and Stoyka Netcheva for home base logistical support. We thank Suncor and its project team (Dan Burt et. al.), AECOM (April Kliachik, Peter Tkalec) and SGS (Nathan Grey, Ardan Ross) for site logistics support. This work was partially funded under the Oil Sands Monitoring Program and is a contribution to the Program but does not necessarily reflect the position of the Program. We also acknowledge funding from the Program for Energy Research and Development (NRCan) and from the Climate Change and Air Quality Program (ECCC).

References

- Alberta Energy Regulator, Directive 085, Fluid Tailings Management for Oil Sands Mining Projects. (2017).
490 <https://www.aer.ca/documents/directives/Directive085.pdf> (last accessed: Oct 21st, 2019)
- Alberta Environment and Parks: Quantification of area fugitive emissions at oil sands mines.
<https://open.alberta.ca/publications/quantification-of-area-fugitive-emissions-at-oil-sands-mines-version-2-0>, 2014
(last accessed: Dec 3, 2019).
- Bari, M. A., and Kindzierski, W. B.: Ambient volatile organic compounds (VOCs) in communities of the Athabasca
495 oil sands region: Sources and screening health risk assessment, *Environ. Pollut.*, 235, 602-614,
<http://doi.org/10.1016/j.envpol.2017.12.065>, 2018.
- Bolinus, D. J., Jahnke, A., and MacLeod, M.: Comparison of eddy covariance and modified Bowen ratio methods
for measuring gas fluxes and implications for measuring fluxes of persistent organic pollutants, *Atmos. Chem.
Phys.*, 16, 5315-5322, <http://doi.org/10.5194/acp-16-5315-2016>, 2016.

- 500 Businger, J. A., Wyngaard, J. C., Izumi, Y., and Bradley, E. F.: Flux- profile relationships in the atmospheric surface layer, *J. Atmos. Sci.*, 28, 181-189, 1971.
- Covey, K. R., and Megonigal, J. P.: Methane production and emissions in trees and forests, *New Phytol.*, 222, 35-51, <http://doi.org/10.1111/nph.15624>, 2019.
- Dyer, A. J., and Hicks, B. B.: Flux-gradient relationships in the constant flux layer, *Quarterly Journal of the Royal Meteorological Society*, 96, 715-721, <http://doi.org/10.1002/qj.49709641012>, 1970.
- 505 Erkkilä, K. M., Ojala, A., Bastviken, D., Biermann, T., Heiskanen, J., Lindroth, A., Peltola, O., Rantakari, M., Vesala, T., and Mammarella, I.: Methane and carbon dioxide fluxes over a lake: Comparison between eddy covariance, floating chambers and boundary layer method, *Biogeosciences*, 15, 429-445, <http://doi.org/10.5194/bg-15-429-2018>, 2018.
- 510 [Fan, S. M., Wofsy, S. C., Bakwin, P. S., Jacob, D. J. and Fitzjarrald, D. R. Atmosphere-biosphere exchange of CO₂ and O₃ in the Central Amazon Forest. *J. Geophys. Res.*, 95: 16851-16864, 1990.](#)
- Flesch, T. K., Wilson, J. D., and Yee, E.: Backward-time Lagrangian stochastic dispersion models and their application to estimate gaseous emissions, *J. Appl. Meteorol.*, 34, 1320-1332, 1995.
- Flesch, T. K., Prueger, J. H., and Hatfield, J. L.: Turbulent Schmidt number from a tracer experiment, *Agric. For. Meteorol.*, 111, 299-307, [https://doi.org/10.1016/S0168-1923\(02\)00025-4](https://doi.org/10.1016/S0168-1923(02)00025-4), 2002.
- 515 Flesch, T. K., Wilson, J. D., Harper, L. A., Crenna, B. P., and Sharpe, R. R.: Deducing ground-to-air emissions from observed trace gas concentrations: A field trial, *J. Appl. Meteorol.*, 43, 487-502, 2004.
- Foght, J. M., Gieg, L. M., and Siddique, T.: The microbiology of oil sands tailings: Past, present, future, *FEMS Microbiol. Ecol.*, 93, <http://doi.org/10.1093/femsec/fix034>, 2017.
- 520 Foken, T., Aubinet, M., and Leuning, R.: Eddy Covariance: A practical guide to measurement and data analysis, Eddy covariance method, edited by: Aubinet, M., Vesala, T., and Papale, D., Springer, 438 pp., 2012.
- Galarneau, E., Hollebone, B. P., Yang, Z., and Schuster, J.: Preliminary measurement-based estimates of PAH emissions from oil sands tailings ponds, *Atmos. Environ.*, 97, 332-335, <http://doi.org/10.1016/j.atmosenv.2014.08.038>, 2014.
- 525 Government of Alberta, Lower Athabasca Region – Tailings management framework for the minable Athabasca Oil Sands. 2015. <https://open.alberta.ca/dataset/962bc8f4-3924-46ce-baf8-d6b7a26467ae/resource/7c49eb63-751b-49fd-b746-87d5edee3131/download/2015-larp-tailingsmgatathabascaoilsands.pdf>. (last accessed: Oct 21st, 2019)
- Government of Alberta, Specified gas reporting standard. 2019 Version 11.0 <https://open.alberta.ca/dataset/c5471471-79a3-456b-a183-997692da2576/resource/14073f8c-deab-410e-a9ab-ed326e5e4052/download/specified-gas-reporting-standard-v-11.pdf>. (last accessed: Oct 21st, 2019)
- 530 Government of Canada Greenhouse Gas Reporting Program, <https://climate-change.canada.ca/facility-emissions/GHGRP-G10558-2017.html>. 2017. (last accessed: Dec 4th, 2019)

Field Code Changed

- Gualtieri, C., Angeloudis, A., Bombardelli, F., Jha, S., and Stoesser, T.: On the Values for the Turbulent Schmidt Number in Environmental Flows, *Fluids*, 2, <http://doi.org/10.3390/fluids2020017>, 2017.
- 535 Hashmonay, R. A., Natschke, D. F., Wagoner, K., Harris, D. B., Thompson, E. L., and Yost, M. G.: Field evaluation of a method for estimating gaseous fluxes from area sources using open-path fourier transform infrared, *Environ. Sci. Tech.*, 35, 2309-2313, <http://doi.org/10.1021/es0017108>, 2001.
- Horst, T. W.: The footprint for estimation of atmosphere-surface exchange fluxes by profile techniques, *Bound-Lay. Meteorol.*, 90, 171-188, 1999.
- 540 Kljun, N., Calanca, P., Rotach, M. W., and Schmid, H. P.: A simple two-dimensional parameterisation for Flux Footprint Prediction (FFP), *Geosci. Model Dev.*, 8, 3695-3713, <http://doi.org/10.5194/gmd-8-3695-2015>, 2015.
- Kong, J. D., Wang, H., Siddique, T., Foght, J., Semple, K., Burkus, Z., and Lewis, M. A.: Second-generation stoichiometric mathematical model to predict methane emissions from oil sands tailings, *Sci. Total Environ.*, 694, 133645, <https://doi.org/10.1016/j.scitotenv.2019.133645>, 2019.
- 545 Li, S. M., Leithead, A., Moussa, S. G., Liggio, J., Moran, M. D., Wang, D., Hayden, K., Darlington, A., Gordon, M., Staebler, R., Makar, P. A., Stroud, C. A., McLaren, R., Liu, P. S. K., O'Brien, J., Mittermeier, R. L., Zhang, J., Marson, G., Cober, S. G., Wolde, M., and Wentzell, J. J. B.: Differences between measured and reported volatile organic compound emissions from oil sands facilities in Alberta, Canada, *Proc. Natl. Acad. Sci. U. S. A.*, 114, E3756-E3765, <http://doi.org/10.1073/pnas.1617862114>, 2017.
- 550 Liggio, J., Li, S. M., Staebler, R. M., Hayden, K., Darlington, A., Mittermeier, R. L., O'Brien, J., McLaren, R., Wolde, M., Worthy, D., and Vogel, F.: Measured Canadian oil sands CO₂ emissions are higher than estimates made using internationally recommended methods, *Nat. Commun.*, 10, <http://doi.org/10.1038/s41467-019-09714-9>, 2019.
- Liggio, J., Moussa, S. G., Wentzell, J., Darlington, A., Liu, P., Leithead, A., Hayden, K., O'Brien, J., Mittermeier, R. L., Staebler, R., Wolde, M., and Li, S. M.: Understanding the primary emissions and secondary formation of gaseous organic acids in the oil sands region of Alberta, Canada, *Atmos. Chem. Phys.*, 17, 8411-8427, <http://doi.org/10.5194/acp-17-8411-2017>, 2017.
- [Mauder, M. and Foken, T.: Documentation and instruction manual of the eddy covariance software package TK2. https://core.ac.uk/download/pdf/33806389.pdf, 2004.](https://core.ac.uk/download/pdf/33806389.pdf)
- 560 Mauder, M., Liebethan, C., Göckede, M., Leps, J-P, Beyrich, F., and Foken, T.: Processing and quality control of flux data during LITFASS-2003, *Bound-Lay. Meteorol.*, 121, 67-88, <http://doi.org/10.1007/s10546-006-9094-0>, 2006.
- Meyers, T. P., Hall, M. E., Lindberg, S. E., and Kim, K.: Use of the modified bowen-ratio technique to measure fluxes of trace gases, *Atmos. Environ.*, 30, 3321-3329, [https://doi.org/10.1016/1352-2310\(96\)00082-9](https://doi.org/10.1016/1352-2310(96)00082-9), 1996.
- 565 Moussa, S.G., Staebler, R.M., You, Y., Leithead, A., Yousif, M.A., Brickell, P., Beck, J. Jiang, Z., Li, S.-M., Liggio, J., Wren, S.N., Darlington, A., and Narayan, J.: Fugitive Emissions of Volatile Organic Compounds from a Tailings Pond in the Oil Sands Region of Alberta. In review, *Env. Sci. Tech.*, 2020a.

- Moussa, S.G., Staebler, R.M. You, Y., Leithead, A., Mittermeier, R., Hayden, K., Mihele, C., and Beck, J.: Total Reduced Sulfur Fugitive Emissions from an Oil Sands Tailings Pond: Sources and Estimates. In review, *Atmos. Env.*, 2020b.
- 570 Myhre, G., Shindell, D., Bréon, F.-M., Collins, W., Fuglestvedt, J., Huang, J., Koch, D., Lamarque, J.-F., D. Lee, B. M., Nakajima, T., Robock, A., Stephens, G., Takemura, T., and Zhang, H.: Anthropogenic and Natural Radiative Forcing. In: *Climate change 2013: The physical science basis: Working Group I contribution to the fifth assessment report of the Intergovernmental Panel on Climate Change*, in, edited by: Stocker, T. F., D. Qin, G.-K. Plattner, M. Tignor, S.K. Allen, J. Boschung, A. Nauels, Y. X., Bex, V., and Midgley, P. M., Cambridge University Press,
- 575 Cambridge, United Kingdom and New York, NY, USA., Chapter 8, Section 8.7, 659-740, 2013.
- Penner, T. J., and Foght, J. M.: Mature fine tailings from oil sands processing harbour diverse methanogenic communities, *Can. J. Microbiol.*, 56, 459-470, <http://doi.org/10.1139/W10-029>, 2010.
- Podgrajsek, E., Sahlée, E., Bastviken, D., Holst, J., Lindroth, A., Tranvik, L., and Rutgersson, A.: Comparison of floating chamber and eddy covariance measurements of lake greenhouse gas fluxes, *Biogeosciences*, 11, 4225-4233,
- 580 <http://doi.org/10.5194/bg-11-4225-2014>, 2014.
- Rooney, R. C., Bayley, S. E., and Schindler, D. W.: Oil sands mining and reclamation cause massive loss of peatland and stored carbon, *Proc. Natl. Acad. Sci. U. S. A.*, 109, 4933-4937, <http://doi.org/10.1073/pnas.1117693108>, 2012.
- Prajapati, P., and Santos, E. A.: Comparing methane emissions estimated using a backward-Lagrangian stochastic model and the eddy covariance technique in a beef cattle feedlot, *Agric. For. Meteorol.*, 256-257, 482-491, <https://doi.org/10.1016/j.agrformet.2018.04.003>, 2018.
- 585 Salloum, M. J., Dudas, M. J., and Fedorak, P. M.: Microbial reduction of amended sulfate in anaerobic mature fine tailings from oil sand, *Waste Manage. Res.*, 20, 162-171, <http://doi.org/10.1177/0734242X0202000208>, 2002.
- Schmid, H. P.: Source areas for scalars and scalar fluxes, *Bound-Lay. Meteorol.*, 67, 293-318,
- 590 <http://doi.org/10.1007/BF00713146>, 1994.
- Schubert, C. J., Diem, T., and Eugster, W.: Methane emissions from a small wind shielded lake determined by eddy covariance, flux chambers, anchored funnels, and boundary model calculations: A comparison, *Environ. Sci. Tech.*, 46, 4515-4522, <http://doi.org/10.1021/es203465x>, 2012.
- Siddique, T., Fedorak, P. M., MacKinnon, M. D., and Foght, J. M.: Metabolism of BTEX and Naphtha Compounds to Methane in Oil Sands Tailings, *Environmental Science & Technology*, 41, 2350-2356, <http://doi.org/10.1021/es062852q>, 2007.
- 595 Siddique, T., Gupta, R., Fedorak, P. M., MacKinnon, M. D., and Foght, J. M.: A first approximation kinetic model to predict methane generation from an oil sands tailings settling basin, *Chemosphere*, 72, 1573-1580, <https://doi.org/10.1016/j.chemosphere.2008.04.036>, 2008.

- 600 Siddique, T., Penner, T., Semple, K., and Foght, J. M.: Anaerobic biodegradation of longer-chain n-alkanes coupled to methane production in oil sands tailings, *Environ. Sci. Tech.*, 45, 5892-5899, <http://doi.org/10.1021/es200649t>, 2011.
- Siddique, T., Penner, T., Klassen, J., Nesbø, C., and Foght, J. M.: Microbial communities involved in methane production from hydrocarbons in oil sands tailings, *Environ. Sci. Tech.*, 46, 9802-9810, <http://doi.org/10.1021/es302202c>, 2012.
- 605 Simpson, I. J., Blake, N. J., Barletta, B., Diskin, G. S., Fuelberg, H. E., Gorham, K., Huey, L. G., Meinardi, S., Rowland, F. S., Vay, S. A., Weinheimer, A. J., Yang, M., and Blake, D. R.: Characterization of trace gases measured over Alberta oil sands mining operations: 76 speciated C₂-C₁₀ volatile organic compounds (VOCs), CO₂, CH₄, CO, NO, NO₂, NO_y, O₃ and SO₂, *Atmos. Chem. Phys.*, 10, 11931-11954, <http://doi.org/10.5194/acp-10-11931-2010>, 2010.
- 610 Small, C. C., Cho, S., Hashisho, Z., and Ulrich, A. C.: Emissions from oil sands tailings ponds: Review of tailings pond parameters and emission estimates, *Journal of Petroleum Science and Engineering*, 127, 490-501, <http://doi.org/10.1016/j.petrol.2014.11.020>, 2015.
- Stantec: Air pollutant and GHG emissions from mine faces and tailings ponds, 413, 2016.
- 615 Statutes of Alberta, Oil sands emissions limit act Chapter O-7.5 (2016). <http://www.qp.alberta.ca/documents/Acts/O07p5.pdf>. (last accessed: Oct 21st, 2019)
- Strawbridge, K. B., Travis, M. S., Firanski, B. J., Brook, J. R., Staebler, R., and Leblanc, T.: A fully autonomous ozone, aerosol and nighttime water vapor lidar: a synergistic approach to profiling the atmosphere in the Canadian oil sands region, *Atmos. Meas. Tech.*, 11, 6735-6759, <http://doi.org/10.5194/amt-11-6735-2018>, 2018.
- 620 Stull, R. B.: Chapter 6.4 Local Closure – First Order, in: *An Introduction To Boundary Layer Meteorology*, Kluwer Academic Publishers, Netherland, 203-214, 2003a.
- Stull, R. B.: Chapter 5 Turbulence Kinetic Energy, Stability and Scaling, in: *An Introduction To Boundary Layer Meteorology*, Kluwer Academic Publishers, Netherland, 182, 2003b.
- [Wilczak, J. M., Oncley S. P., and Stage, S.A.: Sonic anemometer tilt correction algorithms. *Bound-Lay. Meteorol.*, <http://doi.org/10.1023/A:1018966204465>, 99, 127-150, 2001.](http://doi.org/10.1023/A:1018966204465)
- 625 Wolf, A., Saliendra, N., Akshalov, K., Johnson, D. A., and Laca, E.: Effects of different eddy covariance correction schemes on energy balance closure and comparisons with the modified Bowen ratio system, *Agric. For. Meteorol.*, 148, 942-952, <http://doi.org/10.1016/j.agrformet.2008.01.005>, 2008.
- Xiao, W., Liu, S., Li, H., Xiao, Q., Wang, W., Hu, Z., Hu, C., Gao, Y., Shen, J., Zhao, X., Zhang, M., and Lee, X.: A flux-gradient system for simultaneous measurement of the CH₄, CO₂, and H₂O fluxes at a lake-air interface, *Environ. Sci. Tech.*, 48, 14490-14498, <http://doi.org/10.1021/es5033713>, 2014.
- 630

Yeh, S., Jordaan, S. M., Brandt, A. R., Turetsky, M. R., Spatari, S., and Keith, D. W.: Land use greenhouse gas emissions from conventional oil production and oil sands, *Environ. Sci. Tech.*, 44, 8766-8772, <http://doi.org/10.1021/es1013278>, 2010.

635 You, Y., Staebler, R. M., Moussa, S. G., Su, Y., Munoz, T., Stroud, C., Zhang, J., and Moran, M. D.: Long-path measurements of pollutants and micrometeorology over Highway 401 in Toronto, *Atmos. Chem. Phys.*, 17, <http://doi.org/14119-14143>, 10.5194/acp-17-14119-2017, 2017.

You, Y., Moussa, S. G., Zhang, L., Fu, L., Beck, J., Staebler, R. M.: Determining gas emissions from an oil sands tailings pond with open-path FTIR measurements, In review, *Atmos. Chem. Phys.*, 2020.

640 Zhang, L., Cho, S., Hashisho, Z., and Brown, C.: Quantification of fugitive emissions from an oil sands tailings pond by eddy covariance, *Fuel*, 237, 457-464, <http://doi.org/10.1016/j.fuel.2018.09.104>, 2019.

Zhao, J., Zhang, M., Xiao, W., Wang, W., Zhang, Z., Yu, Z., Xiao, Q., Cao, Z., Xu, J., Zhang, X., Liu, S., and Lee, X.: An evaluation of the flux-gradient and the eddy covariance method to measure CH₄, CO₂, and H₂O fluxes from small ponds, *Agric. For. Meteorol.*, 275, 255-264, <http://doi.org/10.1016/j.agrformet.2019.05.032>, 2019.

Tables

Table 1 Summary of CH₄ fluxes (g m⁻² d⁻¹) in this study.

Flux method	Q_25%	median	Q_75%	mean ^c
EC ^a	4.2	5.9	7.9	6.1 ± 0.5
Gradient ^a	2.6	4.6	7.9	5.7 ± 1.6
IDM ^a	3.6	5.2	6.6	5.4 ± 0.4
Flux Chamber ^b	2.0	2.3	3.8	2.8 ± 1.4 ^d

^a Statistics and average fluxes are area weight-averaged.

^b Statistics and average of 15 measurements described in Section 4.6.

^c Errors with the mean fluxes are calculated with a “top-down” error estimation approach, using the average of standard deviations of fluxes from five periods when the fluxes displayed high stationarity.

^d The error is the standard deviation of the 15 measurements. Emission estimates were 5.3 g m⁻² d⁻¹ in 2016 and 11.1 g m⁻² d⁻¹ in 2018.

Deleted: were relatively steady.

Table 2 Comparison of CH₄ fluxes (g m⁻² d⁻¹) in this study to previously reported fluxes.

	TAPOS(2017)	Small et al. (2015) ^a	Stantec report (2016)		Baray et al. (2018) ^b	Flux Chamber 2017	
				bubbling zones	quiescent zones		
CH ₄	6.1 (EC)	2.6	2013	12.9	2.1	17.1	2.8
			2014	9.6	BDL		
CO ₂	18.0 (EC)	16.4	2013	14.9	10.5	NA	21.2
			2014	11.0	BDL		

^a The original units are tonnes hectare⁻¹ year⁻¹. Measurements were taken from August to October in 2010 or 2011. The pond area was 2.8 km² as listed in Table 1 of Small et al. (2015). We assumed no seasonal variations to extrapolate from summer measurements to annual totals.

^b The original number is 2.0 tonnes hour⁻¹, and the pond water surface area was 2.8 km² (Small et al, 2015).

Figures



Figure 1: Overall map of the study site and close-up of the pond in September 2017. The superimposed polar plot shows the footprints under unstable conditions. Two traces in the polar plot show the medians of 80% and 50% contribution distances (in meters) for the measured half-hour periods EC fluxes in 16 wind direction bins. Angles in the polar plot are the wind direction (true North) with the center at the main site. The 15 white circles on the surface of the pond indicate the locations of the flux chamber measurements. The grey areas north of the r=1000m circle are sandy deposits; dark grey represents liquid surfaces.

Deleted: 2017

Deleted: label

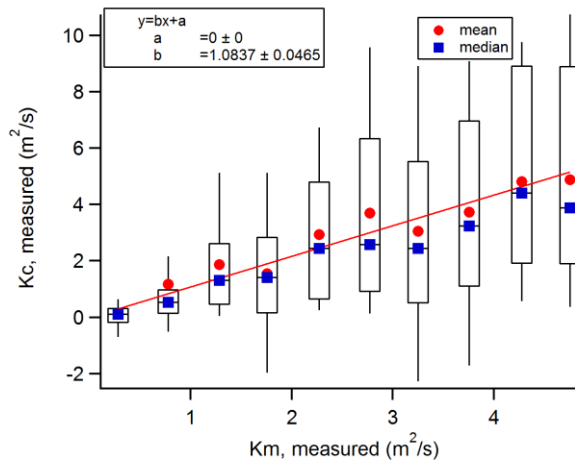


Figure 2: Calculating Schmidt Number S_c as a constant over the entire study. Lower and upper bounds of the box are 25th and 75th percentile of each bin; the lines in the box and the blue squares mark the median; red circle labels the mean of data in each bin; whiskers are 10th and 90th percentile of data.

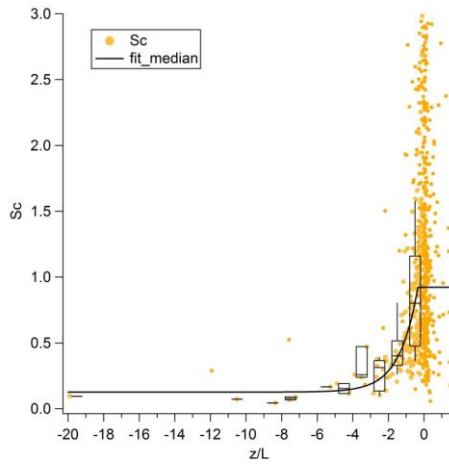


Figure 3: Dependence of S_c on z/L measured at 18m. Yellow points are S_c observed in each individual half-hour period when the wind was from the pond; the black curve is the best fit of S_c versus median z/L from each z/L bin. In this analysis, S_c was binned by z/L with bin width=1 before fitting.

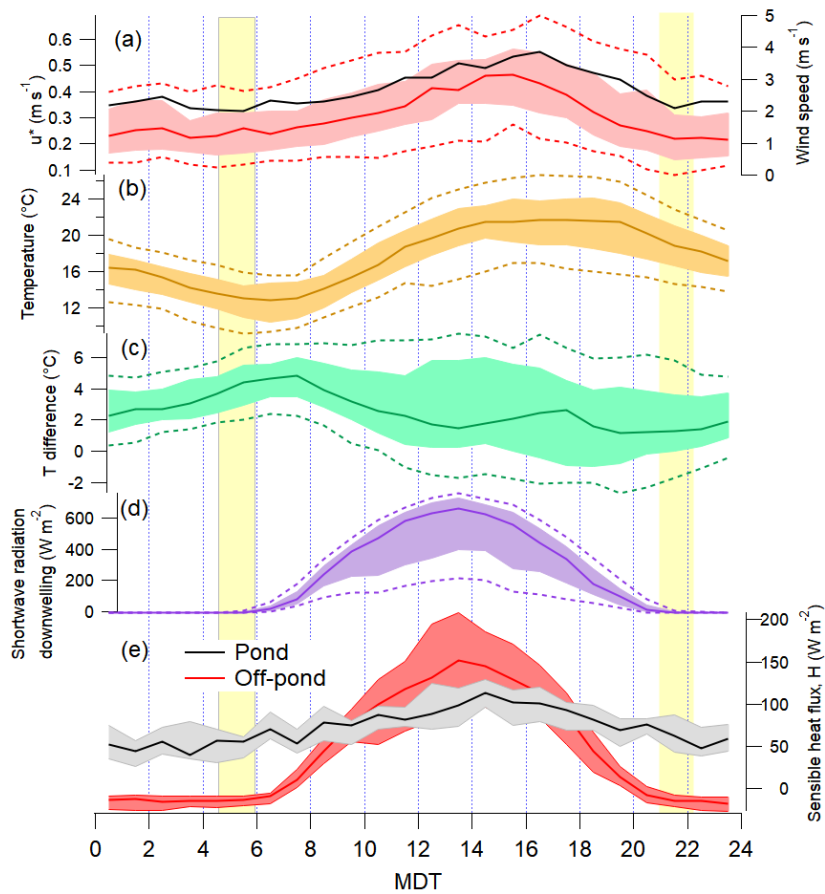


Figure 4: Diurnal variations of (a) u^* at 8m (red) and wind speed at 4m (black); (b) ambient temperature at 8m; (c) the temperature difference between the surface of the pond and the ambient temperature at 8m; (d) downwelling shortwave radiation; (e) the sensible heat flux at 8m. Solid lines show the median; shades indicate the interquartile ranges; and dashed lines label 10th and 90th percentiles. MDT denotes Mountain Daylight Savings Time (hours). The yellow shades mark the range of local sunrise and sunset time during this 5-week project.

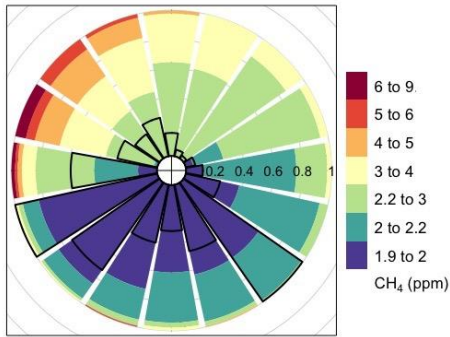


Figure 5: Rose plot of CH_4 mole fraction at 18m. Colors represent CH_4 mole fraction. The length of each colored segment represents the time fraction of that mole fraction range in each direction bin. The radius of the black open sectors indicates the frequency of wind in each direction bin; angle represents wind direction, straight up is the North, straight left is the West.

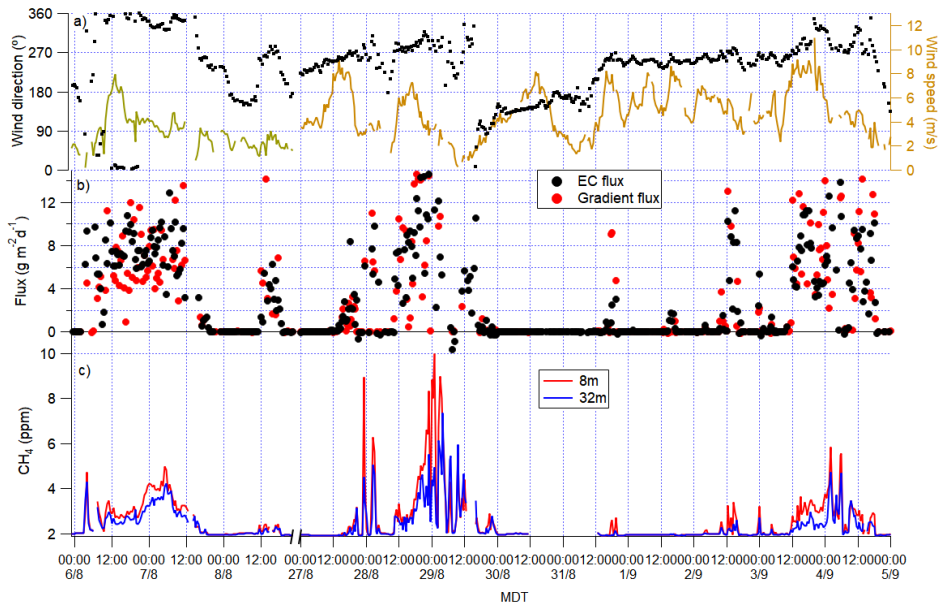


Figure 6: Time series of (a) wind direction, wind speed, (b) CH_4 EC fluxes and gradient fluxes, and (c) CH_4 mole fractions at 8m and 32m, from Aug 6th to 9th, and from Aug 27 to Sep 5.

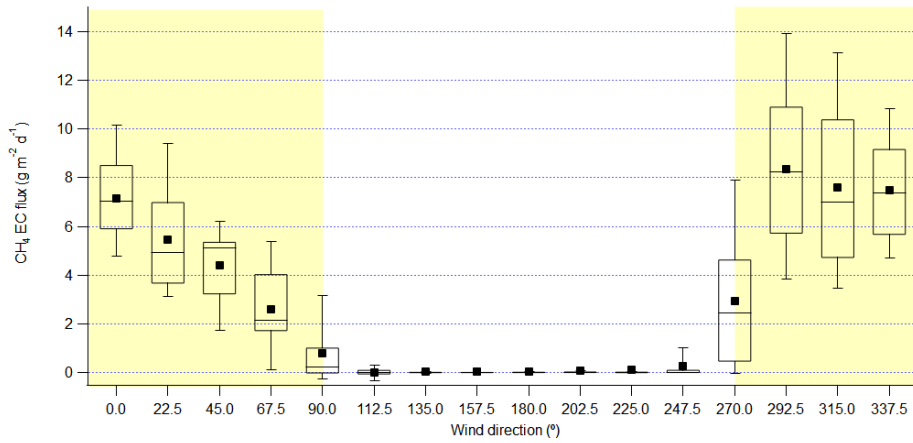


Figure 7: EC flux of CH₄ as a function of wind direction binned in 22.5-degree bins. Lower and upper bounds of the box plot are 25th and 75th percentile; the line in the box marks the median and the black square labels the mean; the whiskers label the 10th and 90th percentile. Yellow shades indicate the wind directions from the pond.

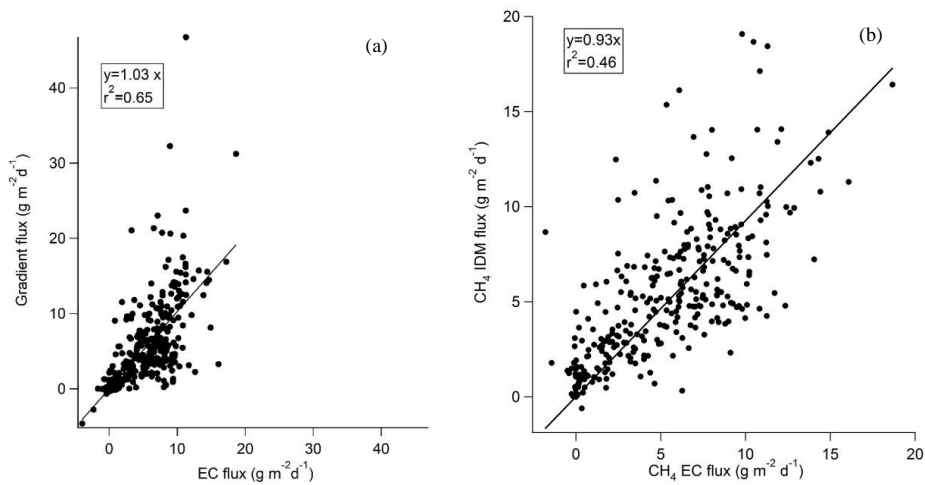


Figure 8: CH₄ gradient flux (a) and IDM flux (b) compared with EC flux.